universität wien

MASTERARBEIT /MASTER'S THESIS

Titel der Masterarbeit / Title of the Master's Thesis

„Proteomics-based characterization of Alzheimer's disease and gender-related platelet protein biomarkers“

verfasst von / submitted by

Ina Dhrami, BSc

angestrebter akademischer Grad / in partial fulfillment of the requirements for the degree of

Master of Science (MSc)

Wien, 2020 / Vienna 2020

Studienkennzahl lt. Studienblatt / degree programme code as it appears on the student record sheet:	UA 066 834
Studienrichtung lt. Studienblatt / degree programme as it appears on the student record sheet:	Masterstudium Molekulare Biologie
Betreut von / Supervisor:	Univ. Prof in. Dr. in med.univ. Margarethe Geiger

I. ACKNOWLEDGEMENTS

I would like to give my thanks to Prof[in]. Margarethe Geiger and Dr Maria Zellner for allowing me to accomplish my master thesis in their research facility.

I would also like to express my sincere thanks to Huriye Ercan, MSc. for being the second reader of my thesis. You were the best colleague I could ever wish for which I enjoyed working with and a dear friend in good and hard times.

I am extremely blessed and grateful for my mother Kostandina, my sister Dori and my best friend Ana for always believing in me. Without their constant emotional support and encouragement, I wouldn't have gotten this far in life.

II. TABLE OF CONTENTS

III. ABBREVIATIONS

1-ANOVA	One-way analysis of variance
1D	One-dimensional
2-ANOVA	Two-way analysis of variance
2D	Two-dimensional
2D-DIGE	Two-dimensional differential in-gel electrophoresis
AChEIs	Acetylcholinesterase inhibitors
AD	Alzheimer's disease
APOE	Apolipoprotein E
APP	Amyloid precursor protein
APS	Ammonium persulfate
Aβ	Amyloid beta protein
BBB	Blood-brain barrier
BSA	Bovine serum albumin
BVA	Biological Variation Analysis
CERAD	Consortium to Establish a Registry for Alzheimer's disease
CSF	Cerebrospinal fluid
CT	Computed tomography
ddH_2O	Milli-Q water
DIA	Differential In-Gel Analysis
DLB	Dementia with Lewy Bodies
DMF	Dimethylformamide
DPBS	Dulbecco´s Phosphate Buffered Saline
DTT	1,4-Dithiothreitol
EOAD	Early-onset AD
FAD	Familial form of AD
FDG	2-[18F] fluoro-2-deoxy-D-glucose
GAPDH	Glyceraldehyde-3-phosphate dehydrogenase
GDI1	Rab GDP dissociation inhibitor alpha
GFP	Gel filtered platelets
GMPR	GMP reductase 1
GPx	Glutathione peroxidases

GPX1	Glutathione peroxidase 1
GSH	Glutathione
HCl	Hydrochloric acid
IAA	Iodoacetamide
IEF	Isoelectric focusing
IHC	Immunohistochemistry
IPG	Immobilized pH gradient strip
IS	Internal standard
kDa	Kilodalton
LOAD	Late-onset AD
LTB	Lower Tris Buffer
MAP	Microtubule-associated protein
MARK	Microtubule affinity-regulating kinase
MCI	Mild cognitive impairment
MK	Megakaryocytes
MMSE	Mini-Mental State Examination
MRI	Magnetic resonance imaging
mRNAs	Messenger RNAs
MS	Mass Spectrometry
MSA	Multiple systems atrophy
MSN	Moesin
MT	Microtubule
MW	Molecular Weight
NFTs	Neurofibrillary tangles
NINCDS-ADRDA	National Institute of Neurological and Communicative Disorders and Stroke and the Alzheimer's Disease and Related Disorders Association
NMDA	N-Methyl-D-aspartate Receptor
NrCAM	Neuronal cell adhesion molecule
PAF	Pure autonomic failure
PD	Parkinson disease
PDD	PD dementia
PET	Positron emission tomography
PHF	Paired helical filaments

pI	Isoelectric point
PMT	Photomultiplier
PRP	Platelet-rich plasma
PSEN1	Presenilin 1
PSEN2	Presenilin 2
P-tau	Phosphorylated tau
r^2	Pearson correlation coefficient
rpm	Rounds per minute
RuBPS	Tris (bathophenanthroline disulfonate) ruthenium (II) sodium salt
SA	Standardized abundance
SDS	Sodium dodecyl sulfate-polyacrylamide
SLAB	SDS loading buffer
SNCA	Alpha-synuclein
SOD1	Superoxide dismutase 1
sRNAs	Small RNAs
TCA	Trichloroacetic acid
TEMED	Tetramethylethylendiamine
T-tau	Total tau
UTB	Upper Tris Buffer
WB	Western blot
YKL-40	Chitinase-3 like-1, human cartilage glycoprotein-39, and chondrex
λ	Wavelengt

IV. ABSTRACT

Alzheimer's disease (AD) is a frequent neurodegenerative disorder of the brain characterized by progressive cognitive impairment and the most common cause of dementia in the elderly. Nowadays, AD is one of the major medical challenges of the century and a worldwide burden for relatives, society and the economy. More than a century after its discovery, the most important hallmarks of AD remain the amyloid plaques consisting of amyloid beta (Aβ) and neurofibrillary tangles (NFTs) arising from hyperphosphorylated tau protein. Yet, no effective treatment against AD is available because the onset of the symptoms becomes evident at a late stage after a long period of clinically silent neurodegeneration. Therefore, elucidating the molecular pathogenesis in the preclinical phase and the detection of reliable biomarkers is of immense relevance for diagnostic and therapeutic development. An additional biological variable that is currently under intense investigation is sex. The necessity to uncover sex differences in AD has immense importance for better patient stratification and more personalized treatments.

This study aimed to identify reliable cognition and sex-related biomarkers in the platelet proteome of mild cognitive impairment (MCI) and AD patients by two-dimensional differential in-gel electrophoresis (2D-DIGE) and mass spectrometry (MS). In the pH range 4-7, 115 AD patients (77 females and 38 males), 59 MCI patients (44 females and 15 males) and 157 healthy controls (101 females and 56 males) were analysed. Additionally, 108 AD patients (75 females and 33 males), 43 MCI patients (31 females and 12 males) and 155 healthy controls (101 females and 54 males) were examined in the pH range 6-9. The comparative platelet protein profile revealed 26 significantly altered proteins in both pH ranges from which 7 proteins revealed as promising AD biomarkers. These proteins are involved in signal transduction, vesicle-mediated transport, axonogenesis, co-pathogenic interactions with APOε4, Aβ and tau, antioxidant activity, energy metabolism, cytoskeletal regulation, and nucleotide metabolism. Their cognition and sex-related protein profiles were altered as follows: Rab GDP dissociation inhibitor alpha protein species with a pI 4.50 (+23% in male AD), Alpha-synuclein (+9% in male AD), Superoxide dismutase 1 (+24% in male AD), Glutathione peroxidase 1 (-17% in male AD and -15% in female AD), Glyceraldehyde-3-phosphate dehydrogenase (-23% in female AD), Moesin (+19% in female MCI) and GMP reductase 1 (+12% in female MCI).

These findings give an insight into the complexity of AD as a polyproteinopathy and should help to better understand the underlying molecular mechanism. However, some of these proteins seem to converge at some point in the downstream pathway with other neurodegenerative diseases, therefore more accuracy in finding AD specific biomarkers is needed. Thus, screening the platelet proteome for protein alterations in the preclinical stage in conjunction with an easily accessible, abundant and non-

invasive biomarker source will be crucial for establishing an early diagnosis via blood tests and would help to develop more effective therapies.

V. ZUSAMMENFASSUNG

Alzheimer Krankheit (AD, auch Morbus Alzheimer genannt) ist eine häufige neurodegenerative Erkrankung des Hirnes charakterisiert von einer progressiven kognitiven Beeinträchtigung und ist die häufigste Ursache von Demenz in älteren Menschen. Morbus Alzheimer ist zurzeit einer der größten medizinischen Herausforderungen des Jahrhunderts und eine weltweite Belastung für die Angehörigen, die Gesellschaft und die Wirtschaft. Mehr als ein Jahrhundert nach ihrer Entdeckung, die wichtigsten Anzeichen der Alzheimer Krankheit bleiben die senilen Plaques, bestehend aus Beta-Amyloid-Peptiden und Neurofibrillen, die aus hyperphosphoryliertes Tau-Protein entstehen. Bis zur heutigen Zeit gibt es immer noch keine effektive Therapie gegen der Alzheimer-Krankheit, weil die Symptome erst nach einer langen Phase der klinischen stillen Neurodegeneration auftreten. Deshalb wäre die Aufklärung der molekularen Pathogenese in der präklinischen Phase und die Entdeckung von zuverlässigen Biomarkern von immenser Bedeutung für die Entwicklung von Diagnostik und Therapien. Eine zusätzliche biologische Variable, die zurzeit unter intensive Erforschung steht, ist das Geschlecht. Die Notwendigkeit geschlechtsspezifische Unterschiede in der Alzheimer Krankheit aufzudecken, hat eine sehr wichtige Bedeutung für eine bessere Patientenstratifizierung und personalisierte Behandlung.

Diese Studie diente der Identifikation von zuverlässigen, kognitive und geschlechtsspezifische Biomarkern für Patienten mit einer leichten kognitiven Beeinträchtigung (MCI) sowie Alzheimer-Patienten mittels zweidimensionaler Differentialgelelektrophorese (2D-DIGE) und Massenspektrometrie (MS). Im pH-Bereich 4-7, wurden 115 AD Patienten (77 Frauen und 38 Männer), 59 MCI Patienten (44 Frauen und 15 Männer) und 157 gesunde Kontrollpersonen (101 Frauen und 56 Männer) analysiert. Zusätzlich wurden 108 AD Patienten (75 Frauen und 33 Männer), 43 MCI Patienten (31 Frauen und 12 Männer) und 155 gesunde Kontrollpersonen (101 Frauen und 54 Männer) im pH-Bereich 6-9 untersucht. Das vergleichende Plättchen Protein Profil zeigte 26 signifikant veränderte Proteine in beiden pH-Bereichen von welchen 7 Proteine das Potenzial haben, passende AD Biomarkern zu sein. Diese Proteine sind in Signaltransduktion, Vesikeltransport, Axogenese, pathogene Interaktionen zwischen APOε4, Aβ und Tau-Protein, anti-oxidative Aktivität, Energiestoffwechsel, Regulation des Zytoskeletts und Nukleotidstoffwechsel involviert. Deren kognitive und geschlechtsspezifische Protein Profil verändert sich unterschiedlich, wie Rab GDP dissociation inhibitor

alpha Protein Isoform mit einem pI von 4.50 (+23% in männliche AD Patienten), Alpha-synuclein (+9% in männliche AD Patienten), Superoxide dismutase 1 (+24% in männliche AD Patienten), Glutathione peroxidase 1 (-17% in männliche AD Patienten and -15% in weibliche AD Patientinnen), Glyceraldehyde-3-phosphate dehydrogenase (-23% in weibliche AD Patientinnen), Moesin (+19% in weibliche MCI Patientinnen) und GMP reductase 1 (+12% in weibliche MCI Patientinnen).

Diese Ergebnisse geben ein Einblick in die Komplexität von AD als eine Multiprotein-Krankheit und sollten zu einem besseren Verständnis von den grundlegenden molekularen Mechanismen führen. Allerdings findet man manche dieser Proteine ab einen gewissen Punkt auch in andere neurodegenerative Krankheiten, weswegen die Anforderung zu mehr Präzision beim Ermitteln von AD spezifischen Biomarker ein großer Fortschritt wäre. Die Untersuchung vom Plättchen Proteom nach Protein Veränderungen im präklinischen Stadium in Zusammenhang mit leicht zugängliche, ergiebige, aber nicht invasive Biomarker Quelle, wird deshalb bei der Erstellung einer frühen Diagnose mittels Bluttests entscheidend sein und weiteres bei der Entwicklung effizientere Therapien verhelfen.

1. Introduction

The first case of Alzheimer's disease (AD) was reported in 1907 by Dr Alois Alzheimer, a German neuropathologist and psychiatrist. He described the clinical and pathological features of an unknown brain disease which now bears his name. Since then, our knowledge of understanding the AD pathology has improved immensely but still, there are no disease-modifying treatments. Nowadays, AD has become a worldwide burden of society and one of the major medical challenges of the century. Even the World Health Organisation has recognized AD as a global public health priority [1-3].

1.1 Epidemiology

AD is an age-related neurodegenerative disorder of the brain characterized by progressive cognitive impairment. AD is the biggest cause of dementia and contributes to 50-75% of all cases of dementia. AD and other dementias are an increasing global health challenge with a huge impact on relatives and society [4, 5]. Currently, 40-50 million people are living worldwide with dementia, a global community corresponding to the population of South Korea or Spain. By 2050, the number of dementia patients is likely to rise to 152 million, a global community equivalent to the population of Russia or Bangladesh. The annual cost of this disease is around a trillion US dollars. Worldwide, every three seconds a new case of dementia is diagnosed. In England and Wales, dementia is the number one disease leading to death, globally the 5th [2, 6, 7]. In Austria, AD is the 4th leading cause of death after ischemic heart disease, lung cancer and stroke [8].

1.2 Etiology

AD occurs in two forms, a dominant inhered form (mono-genetic) and a non-dominant form (environmental and polygenetic). Genetic mutations that are associated with a family history of the disease cause a rare (<0.5%) familial form of AD (FAD). Responsible for FAD are missense mutations in three genes amyloid precursor protein (APP), presenilin 1 (PSEN1) and presenilin 2 (PSEN2). These mutations lead to overproduction of Aβ that accumulate and aggregate to amyloid plaques. FAD is also allocated to a variant of early-onset AD (EOAD) due to the decay of cognition at a younger age, typically between 30 and 50 years of age. Another cause for EOAD is Down Syndrome (trisomy 21) because they have three copies of the APP gene. The form that causes the vast majority of AD is known as sporadic or late-onset AD (LOAD). In contrast to EOAD, patients with LOAD develop the disease symptoms later

than 65 years of age. LOAD is caused by a complex interplay between genetic and environmental factors [2, 4, 9]. The strongest genetic risk factor for LOAD is the apolipoprotein E4 (*APOE4*) polymorphism. APOE is mapped on chromosome 19q13 and has three frequent variants *APOE2*, *APOE3* and *APOE4.* APOE is found to be a component of lipoproteins where its function is to deliver cholesterol into the cells by binding to the APOE receptor. The *APOE4* variant has the lowest affinity to this receptor when compared to *APOE43* and *APOE2.* However, particular allele combinations such as ε3/ε4 or ε4/ε4 are known to be risk factors for LOAD. Heterozygote APOε3/ε4 and homozygote APOε4 increase the risk of developing AD by three-fold to eight-fold, respectively. The APOε4/ε4 genotype seems to contribute especially strong to the pathogenesis of LOAD by promoting Aβ deposition and impairing clearance [3, 4, 10, 11]. Genome-wide association studies have detected more than 20 further genetic risk factors, involving endosomal vesicle recycling pathways, cholesterol metabolism, inflammatory pathways and oxidative stress [2, 12]. Epidemiological evidence suggests that low-calorie diets, physical exercise, cognitive stimulation, and higher education accomplishments are protective factors against AD [3]. Other factors such as the ageing process itself [4], sex-related differences [13], mid-life hypertension [14], diabetes [15], ischemic stroke [16] and smoking [17] increase the risk of AD.

1.3 Pathogenesis of Alzheimer's disease

AD is a polyproteinopathy where many proteins, as a result of pathogenic conformations, aggregate separately or together in the brain causing neurodegeneration by synaptic dysfunction and cell death. The hallmarks of AD are the formation of amyloid plaques by Aβ (out of a pathogenic processing of APP) and NFTs arising from hyperphosphorylated tau protein. Increased production of neuronal Aβ followed by decreased clearance along the blood-brain barrier (BBB) in conjunction with a reduced degradation by Aβ-degrading enzymes, results in accumulation and aggregation of Aβ in the brain [2, 11]. Amyloid plaques cause changes in neural activities, synaptic impairment and provoke an immune response from glial cells, which release neurotoxic mediators. Lipid-free APOε4 is supposed to be jointly responsible for the formation of fibrillary amyloid plaques because it forms stable complexes with Aβ. APOε4 also have a 40% less effective clearance rate of Aβ, when compared to APOε3, because of its impaired binding to the APOE receptor [11]. Additionally, it has been hypothesized that brain injury or stress leads to an induced APOE expression in order to repair or remodel the damaged tissue. The consequence of the overproduction of APOE are neurotoxic fragments as a result of proteolytic cleavage, whereas APOε4 is more affected than APOε3. APOε4 fragments target neuronal mitochondria and lead to mitochondrial dysfunction which might be one cause for decreased cerebral glucose metabolism in AD patients. Furthermore, truncated APOε4 and it´s fragments increases tau

phosphorylation and facilitates the neurofibrillary tangles accumulation in the neuronal soma and dendrites. Additionally, Aβ oligomers promote the postsynaptic enrichment of tau in the dendritic spine where it interferes with neurotransmission. Genetic, cell culture and transgenic mice studies have strengthened the hypothesis that Aβ acts upstream of tau although strong evidence is available that tau is a key mediator of both Aβ- and APOε4-dependent pathogenesis [11]. Similarly to tau protein, abnormally modified alpha-synuclein accumulates in Lewy bodies. Up to 50% of the AD patients [18] have aberrant accumulations of the presynaptic protein alpha-synuclein in the dystrophic neurites decorated by Aβ plaques. However, alpha-synuclein does not cause AD but plays an essential role in synucleinopathies such as Parkinson disease (PD) or dementia with Lewy Bodies (DLB). Nonetheless, several studies have reported that alpha-synuclein and Aβ coaggregate but the precise role of alpha-synuclein in amyloid plaque formation is still unclear [18]. Furthermore, Aβ promotes the misfolding and accumulation of alpha-synuclein *in vitro* and *in vivo* [11]. The already identified copathogenic interactions between Aβ, tau, ApoE4, and alpha-synuclein suggest a probable downstream mechanism on which the effects of these proteins congregate. Some convergence points might be mitochondrial dysfunction, epigenetic dysregulation, impaired intracellular transport and downstream signalling pathways (Figure 1) [11, 18, 19].

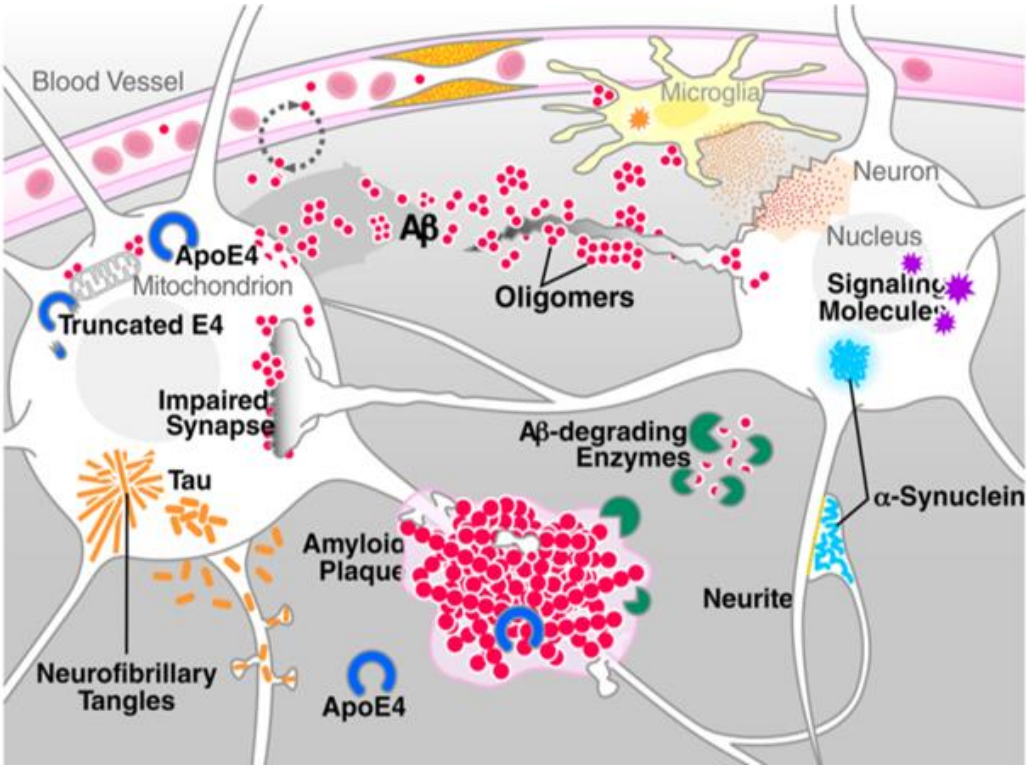

Figure 1: The pathogenesis of AD with its multifactorial features. The interplay of increased Aβ production and impaired clearance leads to accumulation and aggregation of Aβ in the brain. Aβ oligomers compromise synaptic function and its respective signalling pathways. As a response glial cells release neurotoxic mediators. APOε4 whose actual function is to transport lipids into the cell also promotes Aβ deposition and has an impaired clearance of Aβ. Truncated APOε4 is more toxic then APOε4, its fragments impair the mitochondrial function and disturb the cytoskeleton. Hyperphosphorylated tau and alpha-synuclein can self-assemble into NFTs and Lewy bodies respectively causing neurotransmission disruption. Both can spread to other cells by being released into

the extracellular space. **Figure source:** Huang, Y. and L. Mucke, Alzheimer mechanisms and therapeutic strategies. Cell, 2012. **148**(6): p. 1204-22. [11]

1.3.1 Amyloid cascade hypothesis

The Amyloid cascade hypothesis is the most frequent pathophysiological hypothesis of AD. It is based on the abnormal processing and secretion of APP. The uneven levels of Aβ production and clearance is the most significant reason and the triggering event that leads to the pathogenesis of AD. APP has many cleavage sites and undergoes posttranslational proteolytic processing by three enzymes; α-, β-, and γ- secretases. Different proteolytic cleavage of APP by α-γ-secretase (non-amyloidogenic) or β-γ-secretase (amyloidogenic) leads to health conditions or disease (Figure 2). Excessive production of Aβ42/Aβ40 leads to the formation of extracellular amyloid plaques which is one of the hallmarks of AD causing synaptic dysfunction, synapse loss, and finally neuronal death [20-22].

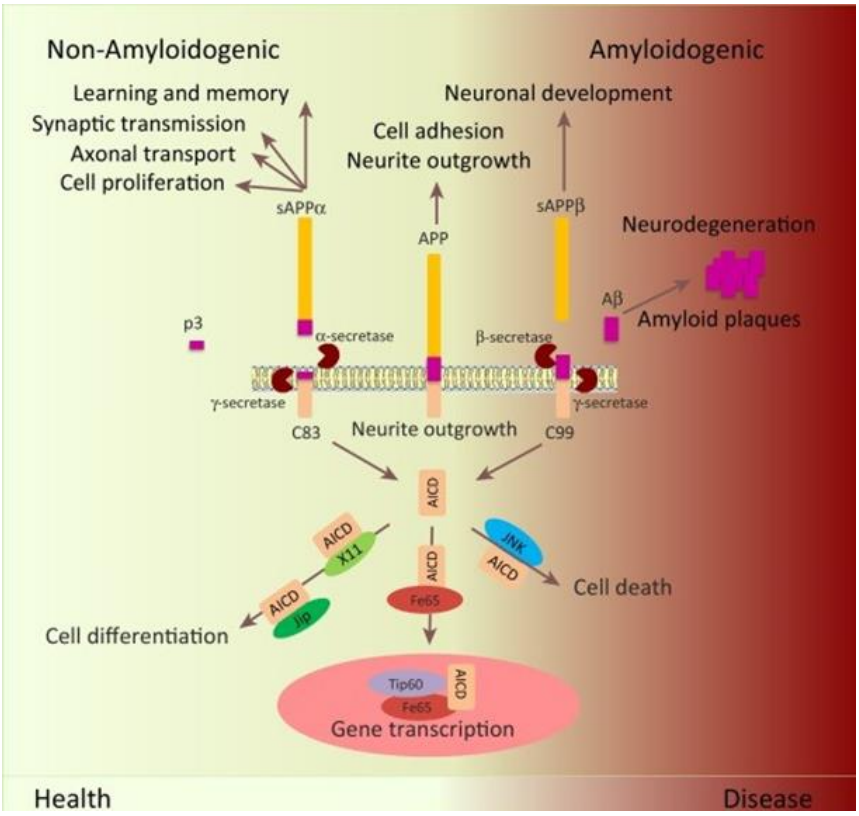

Figure 2: APP proteolytic cleavage pathways in Health and Disease. APP is cleaved by α- β- and γ- secretase. α-secretase cleavage generates soluble sAPPα, which leads to a healthy condition (marked in green) in contrast to β-secretase producing Aβ that leads to amyloid plaque and AD (marked in red). **Figure source:** Deyts, C., G. Thinakaran, and A.T. Parent, APP Receptor? To Be or Not To Be. Trends Pharmacol Sci, 2016. **37**(5): p. 390-411. [21]

1.3.2 Tau hypothesis

Tau is a microtubule-associated protein (MAP) that has six isoforms and more than thirty phosphorylation sites. Tau regulates tubulin binding and assembly into microtubules. Normal tau is necessary for stabilizing microtubule in the cytoskeleton of neurons and neurite outgrowth (Figure 3). Hyperphosphorylated tau dissociates from the microtubule, self-aggregates into paired helical filaments (PHF) and subsequently assembles into NFTs . This event leads to destabilization, impairment and/or interruption of neuronal transport. The consequences are the accumulation of APP, mitochondria, and organelles in the cell body which causes oxidative stress. The amyloid cascade hypothesis suggests that tau is part of a downstream process of Aβ aggregation and toxicity in the pathogenesis of AD. Nevertheless, recent studies indicate that tau pathologies may have, independently of Aβ, a significant role in inducing neurodegeneration. Phosphorylated tau initiates in the entorhinal cortex, in contrast to Aβ depositions which begin in the isocortex. Furthermore, one study reported that Aβ vaccination cleared Aβ, but the advanced tangle pathology remained. Additionally, no clinical improvement was observed. These discoveries give a new perspective on the development of AD therapies by targeting tau pathologies [22-27].

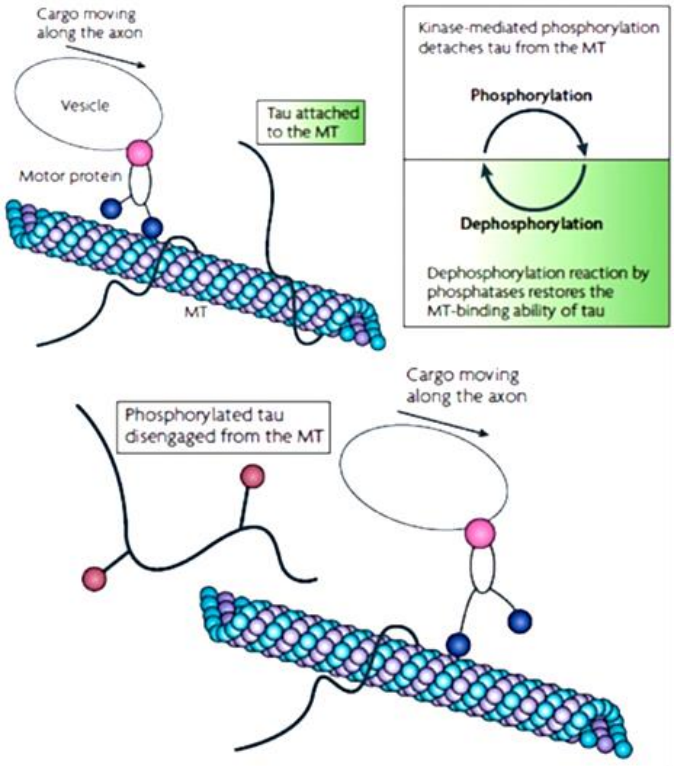

Figure 3: The phosphorylation and dephosphorylation schematic of tau protein. Normal phosphorylated tau dissociates from microtubule (MT) allowing vesicle transport along the axonal MT. Afterwards, dephosphorylation enables tau to bind again to the MT, supporting MT stabilization. In contrast, hyperphosphorylated tau is not able to bind MT but self-aggregate in NFTs. **Figure source:** Schaffer, C., et al., Biomarkers in the Diagnosis and Prognosis of Alzheimer's Disease. J Lab Autom, 2015. 20(5): p. 589-600. [28]

1.3.3 Cholinergic hypothesis

The first and the most studied hypothesis that may cause AD symptoms is the cholinergic hypothesis. The cholinergic hypothesis was defined more than 30 years ago as a degenerative process able of selectively damaging groups of cholinergic neurons in brain regions that have important functional roles in learning, memory, attention and other mnemonic processes [24]. In AD patients, deficits of cholinergic markers such as choline acetyltransferase and acetylcholine were observed. Consequently, it was presumed that the reduction of cholinergic neurons and cholinergic neurotransmission would be followed by cognitive decline. Cholinergic function disturbance correlated to cognitive decline, but no causal connection was detected. Furthermore, medication based on Acetylcholinesterase inhibitors (AChEIs) only temporarily improved the symptoms, indicating a more complex pathophysiology of AD [29].

1.4 Influence of sex differences in the development, symptoms and pathology of Alzheimer's disease

AD is known to be a multifactorial disease with a large diversity in its risk factors, pathophysiological mechanisms, and cognitive syndromes. To develop more accurate diagnosis and treatments in AD, the emphasis on evaluating sex as a biological variable is growing [30, 31]. Recently, consistent evidence revealed that females are at significantly greater risk of developing AD than males [13]. Multiple review papers indicate that two-thirds of clinical AD patients are females [30]. There are differences between males and females in cognitive exhibition and psychiatric symptoms. Studies demonstrate that healthy females perform better than healthy males in the verbal memory domain. Furthermore, the verbal memory is preserved in females with amnestic mild cognitive impairment (MCI) compared to males with the same diagnosis. On the other hand females with AD dementia show lower performance in verbal memory and fluency tasks than males with AD. The available evidence indicates differences in behavioural symptoms between sexes. Males diagnosed with AD display apathy, agitation, and socially inappropriate behaviour while females show depressive symptoms, reclusiveness, emotional lability, delusions, and manic symptoms [31]. Moreover, several studies have shown that the cognitive decline after the diagnosis of MCI and AD is faster in females than in males. The same pattern can be seen in brain atrophy rates in several brain regions. Females with amnestic MCI and AD dementia have a faster atrophy rate (1-1.5% per year) than males [31]. Besides the previously mentioned differences, there is strong evidence that the biggest genetic risk factor for LOAD, namely APOEε4 allele is also sex-dependent. Female ε4 carriers, especially between the ages of 55 and 70 years, have an increased incidence to develop MCI or AD than male ε4 carriers. An explanation for this early susceptibility of

female carriers could be hormonal and metabolic changes occurring early in menopause which interact with the *APOE* genotype to affect AD risk. However, this hypothesis has not yet been investigated, so further studies are required to elucidate this complex interaction. Furthermore, studies of preclinical AD suggest that females who were APOEε4 and Aβ positive show a faster cognitive decline compared with their male counterparts. However, the effects of sex differences on AD epidemiology are now under intense investigation, because the concept of sex-specific clinicopathological AD phenotypes is largely unknown. Elucidating sex-related differences in AD will be crucial for patient stratification, personalized treatment and an additional important factor toward precision medicine [13, 30, 31].

1.5 Diagnostic criteria of Alzheimer's disease

The National Institute of Aging and the International Working Group have recently released new diagnostic criteria where they redefine and expand coverage of the full range of AD stages. The new AD stages are as following:

- Asymptomatic (preclinical AD)
  Includes individuals with biomarkers in evidence of the AD pathology but without clinical symptoms.
- Predementia (MCI due to AD)
  Includes individuals with progressive problems with episodic memory. Subsequently, topographical difficulties, multitasking difficulties and loss of confidence commonly emerge.
- Dementia (due to AD)
  Includes individuals with a progressed condition of cognitive impairment demonstrating itself in difficulties in performing daily life activities which progresses to behavioural changes, impaired mobility, hallucinations and seizures [32, 33].

1.6 Diagnostic methods for Alzheimer's disease

During the past decades, new findings have contributed to a better understanding of the molecular pathogenesis of AD. Still, there is no way to definitively diagnose AD without performing an autopsy. Yet, establishing a diagnosis is complicated and needs a variety of approaches and detection methods. The routine diagnosis of probable LOAD patients is based on the family and medical history, neurophysiological evaluation, blood tests to exclude AD mimicking conditions, brain imaging techniques and fluid biomarkers [2, 34].

- Neurophysiological evaluation

Several neurophysiological tests help to measure the severity of cognitive impairment against age-related standards. The tests are score-based and evaluate general visuospatial domains, memory, language skills, and the ability to complete daily tasks. A wide variety of neurophysiological tests is available such as the Mini-Mental State Examination (MMSE) and the Consortium to Establish a Registry for Alzheimer's Disease (CERAD) test battery [34]. MMSE consists of 30 questions that are totalled up into a single raw score. The test requires six to ten minutes to conduct. A wide range of domains can be accessed with MMSE including language, memory, attention, orientation and visuospatial proficiency. The MMSE has limitations and is not as accurate as the detailed CERAD. Still, MMSE is used in many studies for the classification of cognitively healthy controls and MCI, a state which is described as not normal but also not demented. Additionally, the education level of the patient must be taken into account when interpreting the results of the MMSE test battery [34, 35]. In contrast to MMSE, the accurate CERAD test battery takes approximately one hour and contains several subsets (scores) such as Verbal Fluency (animal naming), Boston Naming (15 items), MiniMental State Exam (serial 7s omitted), Word List Learning, Constructional Praxis, Word List Recall, Word List Recognition (10 original words, 10 foils) and Constructional Praxis recall [36]. The CERAD test battery can differentiate with high accuracy between healthy controls, MCI- and AD- patients and might be the better choice for the neurophysiological evaluation in AD disease [37].

- Brain imaging techniques

Structural neuroimaging techniques like computed tomography (CT) or ideally magnetic resonance imaging (MRI) are recommended for all patients with cognitive impairment to exclude structural abnormities and to provide further diagnostic information [2]. Volumetric measurements of the hippocampus and entorhinal cortex, which are typically affected regions of AD progression, through MRI can be a support in evaluating disease prognosis, especially by hippocampal atrophy in MCI patients [28]. Positron emission tomography (PET) imaging uses radioactive tracers, that bind to molecules which can be metabolized such as glucose, to create a three-dimensional or two-dimensional coloured computerized image of the neural activity of the brain. PET scan can detect changes in metabolism such as glucose metabolism, blood flow, and cellular communication processes [38]. 2-[18F] fluoro-2-deoxy-D-glucose (FDG)-PET imaging measures glucose consumption in the brain. Hypometabolism in the parietal, temporal, and posterior cortices is associated with AD. FDG-PET imaging is highly sensitive for distinguishing AD from healthy controls but it has a mildly lower specificity because of the similar metabolic reductions found in other forms of dementia. Amyloid PET imaging is a new technique that is now available, clinically. Currently, three agents have been approved (florbetapir, flutemetamol and florbetaben) for usage with amyloid PET. All agents bind to fibrillary β-

amyloid and nearly correlate to the concentration of Aβ postmortem. Another new development is tau PET imaging but it still used only for research purposes [2, 28, 38].

- Fluid biomarkers

A Biomarker is an objectively measurable indicator of a normal biological state, pathological processes or responses to medical intervention. Biomarkers are essential for establishing an early diagnosis of AD which would help to develop more effective drugs and establish a personalized medical approach. An ideal fluid biomarker should be reliable, simple to measure, reproducible, easily accessible and have a low production cost [39]. To date, no blood-based AD-specific prognostic or diagnostic biomarker panel is available [2]. Three cerebrospinal fluid (CSF) biomarkers Aβ42, total tau (t-tau), and tau phosphorylated at threonine 181 (p-tau) have been validated as the core biomarkers of the AD pathophysiology and are being progressively used in clinical trials. These biomarkers are also used for the diagnostic approach. A characteristic CSF pattern in AD is a high level of p-tau and t-tau with a low level of Aβ42 [40]. CSF also contains other proteins that are found to be significantly changed statistically between patients groups with different degrees of cognitive impairment, such as chitinase-3 like-1, human cartilage glycoprotein-39, and chondrex (YKL-40), carnosinase I, chromogranin A, and neuronal cell adhesion molecule (NrCAM) [40]. A suitable inflammatory biomarker for AD might be CSF YKL-40 protein. YKL-40 is an astrocyte-derived protein that plays an important role in the brains inflammatory response and tissue remodelling. This protein is found to be highly up-regulated in AD patients [40]. Furthermore, a correlation between amyloid plaque accumulation and plaque-associated activation of the astrocytes was found. Consequently, a combined measurement of Aβ1-42 and YKL-40 might have a prognostic and diagnostic character for the early detection of AD. Although a very promising results, the collection of CSF by lumbar puncture is a relatively invasive procedure in connection with safety concerns [28, 40]. Therefore, less invasive and easy accessible biomarkers such as blood biomarkers are the desired sample material. Numerous plasma proteins, such as growth factors, cytokines, acute-phase proteins, and adhesion molecules, have been identified as possible AD biomarkers candidates. However, AD-related plasma proteins are not consistent in reproducibility. They don't seem to be primarily connected with neurodegeneration but with the secondary inflammatory processes, making them a none reliable nor suitable source for AD research [41].

1.8 Platelets: a biomarker source for Alzheimer's disease

Platelets are known to play a central role in hemostasis and thrombosis, but they are also involved in neuroinflammatory diseases like AD [42]. They are produced in the bone marrow from megakaryocytes (MK) where they undergo a process of fragmentation and are then released into circulation. They are small (1-4μm), exist in resting or active states, have no nucleus but are still capable of protein biosynthesis since they inherit a pool of messenger RNAs (mRNAs), ribosomes, and regulatory small RNAs (sRNAs) from the MK. Once resting platelets are activated, they restructure their cytoskeleton, change their morphology and secrete the content of their granules such as neurotransmitters, cytokines, and chemokines [43, 44]. Platelets shares many biochemical properties with neurons. They both segregate and respond to neurotransmitters. Furthermore, platelets have been used as a model for studying synaptic vesicle metabolism because of their various similarities in secretory pathways and transporters for uptake and packaging. Evidence can be found that platelets are one of the major sources of Aβ in the circulation. Platelets contain a high concentration of APP and possess α-, β- and γ-secretase, so they can produce all the APP metabolites. Studies have been reported that the platelet activation state positively correlates with the rate of cognitive decline in patients with early AD. Patients with amnestic MCI and increased levels of activated platelets were at higher risk to develop AD within three years [43, 45]. Additionally, tau protein which is the second hallmark of AD has been recently detected in the platelets proteome. Furthermore, blood platelets are an easily accessible, minimally invasive and high abundant sample of material source. All the previously mentioned reasons suggest that platelets are an appropriate diagnostic target for investigating the molecular pattern of AD to enable the development of blood test for routine diagnostic of AD, as well as an early targeted treatment AD-related cognitive decay [41].

1.7 Treatment of Alzheimer's disease

To date, no causal therapies that would stop the damage of neurons are available. The complexity of the disease, lack of prognostic and diagnostic blood biomarkers, the relative impermeability of the BBB, high drug costs and time-consuming longitudinal studies are some of the obstacles which make it difficult to develop effective treatments for AD. Currently, four approved drugs are used for the treatment of AD. They temporarily improve the symptoms by trying to counterbalance the neurotransmitter disturbance.

- Acetylcholinesterase inhibitors (AChEIs)

AChEIs such as rivastigmine, galantamine, and donepezil improve the cholinergic transmission by inhibiting the enzyme acetylcholinesterase which degrades acetylcholine between the synaptic cleft. These drugs are approved for the treatment of mild to moderate AD. In the USA donepezil is also approved for the treatment of severe AD. By low dosage, the side effects like gastrointestinal upset or leg cramps are usually well tolerated.

- N-Methyl-D-aspartate Receptor (NMDA) Antagonist

Another option for symptomatic treatment of AD is memantine. This drug is a low-affinity NMDA receptor antagonist, which protects neurons from glutamate excitotoxicity. Memantine is licensed for moderate to severe AD. Studies indicate an improvement in cognition and a reduction of psychological and behavioural symptoms. The side effects of memantine are headache, constipation, confusion, and dizziness [2, 46-48].

1.9 Aim of the study

This study aimed to identify new reliable cognition and sex-specific platelet-derived biomarkers to uncover AD-related protein profiles in the blood and the involvement of platelets in the pathogenesis of MCI and AD. The future perspective is to establish an accurate AD sex-specific prognostic and diagnostic blood biomarker panel that could help develop better therapies and to accomplish a personalized medical approach.

The specific aims were defined as follows:

- Identification of significantly changed proteins in the pH range 4-7 and 6-9 of the platelet proteomes from female and male AD/MCI patients and sex-age- matched healthy controls by two-dimensional differential in-gel electrophoresis (2D-DIGE)
- Identification of the spots of interest (proteins) via mass spectrometry (MS)
- Validation of 2D-DIGE results by semiquantitative 1D and qualitative 2D Western blots

2. Materials and Methods

2.1 Study design

The objective of the study was to identify cognition and sex-related platelet protein changes of AD patients, MCI patients and sex- and age-matched healthy controls by 2D-DIGE in the pH range 4-7 and 6-9. Hence, platelets were collected and isolated from peripheral blood and their proteome was investigated by 2D-DIGE. To evaluate changes between diseased and healthy controls, protein abundance levels between groups were analyzed with the Decyder^{TM} 2D Software. 2D-DIGE gels were silver stained and altered proteins were identified by MS. Afterwards, 2D-DIGE results were validated by semiquantitative one-dimensional (1D) and qualitative two-dimensional (2D) Western blots (WB).

2.1.1 Ethics statement

The Ethics Committee of Vienna approved the conduction of this study (EK 04-070-0604 and EK 09-219-1209), in accordance with the Declaration of Helsinki.

2.1.2 Study participants

All study participants were from Austria and between the ages of 65 and 95. AD patients were recruited from geriatric-, retirement- and nursing homes. MCI patients and healthy controls were chosen from retirement homes, caregivers or spouses of AD patients and by word-of-mouth recommendation. Written informed consent was obtained from all patients before study entry. Altogether, we examined 174 cognitive impaireds (CI) patients and 157 healthy controls in pH range 4-7. Furthermore, 151 CI patients and 155 healthy controls were analysed in pH range 6-9.

Before recruiting, the study participants following exclusion and inclusion criteria had to be fulfilled: Individuals who smoked or took antidepressants were excluded from the study. To measure the cognitive performance, all participants had to complete the CERAD test battery including MMSE [34]. Furthermore, a clinical examination including anamnesis was performed to exclude possible comorbidities that could affect cognitive performance. Clinically suspected AD patients were examined by MRI to exclude structural abnormities such as strokes, tumours, subdural hematoma, and normal pressure hydrocephalus. Diagnosis of probable AD patients was determined by a physician and a psychologist according to the criteria by the US National Institute of Neurological and Communicative Disorders and Stroke and the Alzheimer's Disease and Related Disorders Association (NINCDS-ADRDA)

[49]. The diagnosis of possible MCI patients was established by a physician and a psychologist according to the new criteria of the symposium held in Stockholm [50]. Participants who had in all cognitive domains age-related norms were classified as healthy controls by a physician and a psychologist.

2.2 Sample preparation

The following workflow was performed to obtain the samples from whole blood (Figure 4):

1. Blood collection into 3.8% citrate tubes
2. Generation of platelet-rich plasma (PRP)
3. Extraction of gel filtrated platelets (GFP)
4. Protein precipitation by trichloroacetic acid (TCA)
5. Protein pellet washing
6. Determination of protein concentration

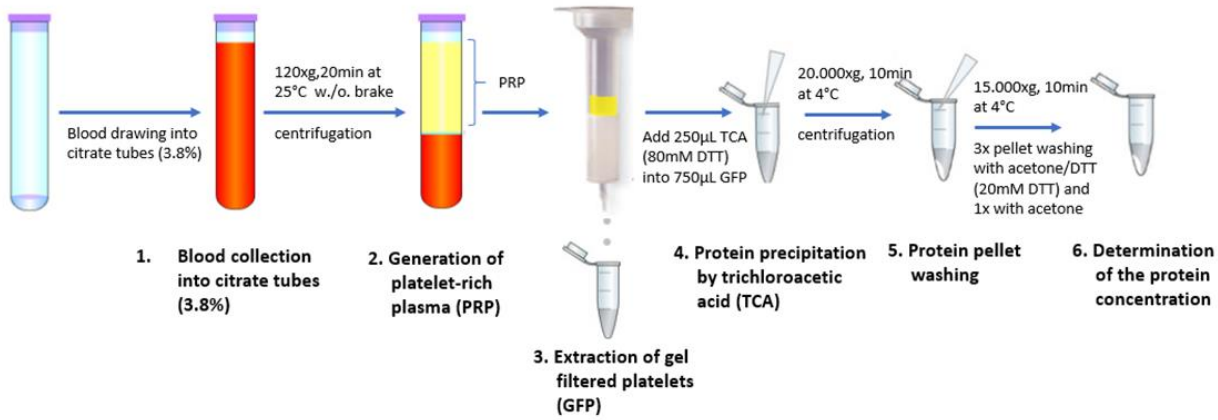

Figure 4: Workflow of platelet isolation from whole blood. PRP: platelet-rich plasma; GFP: gel-filtered-platelets; TCA: trichloroacetic acid; DTT: 1,4-dithiothreitol. This figure was prepared for the present work.

2.2.1 Materials and Solutions

Materials:

1,4-Dithiothreitol (DTT) (Sigma-Aldrich, #11583786001)

6.1N Trichloroacetic acid solution (TCA) (Sigma)

Acetone p.A grade (Merck)

Amberlite IRN-150L (GE Healthcare, #GE17132601)

Bovine serum albumin (BSA) (Sigma-Aldrich, #A7906)

Cell Culture Microplate, 96 Well, F-Bottom (Greiner Bio-One, #651180)

CHAPS (Gerbu, #1083)

Columns for gel filtration – Econo-Pac 15mm diameter (Bio-Rad, USA)

Coomassie Plus Protein Assay Reagent (Pierce, #2326ZZ)

Dulbecco´s Phosphate Buffered Saline (DPBS) (10x) w./o. calcium and magnesium (Gibco, #14200067)

ELISA Reader - Synergy H4 (BioTek)

Hematology cell counter (Sysmex KX-21N)

Sepharose 2B (Sigma-Aldrich, #28-300)

Thiourea (Sigma, #88810)

Tris (Merck, #1.08382)

Urea (GE Healthcare Sigma, #17131901)

Vacuette tube 3.8 % sodium citrate (Greiner Bio-One, #454386)

Solutions:

TCA precipitation

Table 1: Preparation of 4mM DTT working solution

Component	Final concentration	Amount
DTT	4mM	6.17g
ddH_2O		added to 10mL
➢ 20µL, 50µL and 100µL aliquots of 4mM DTT stored at -20 °C		

Table 2: Preparation of TCA (80mM DTT) working solution

Component	Final concentration	Amount
6.1N TCA	80mM	1mL
4mM DTT		20µL

Table 3: Preparation of acetone (20mM DTT) working solution

Component	Final concentration	Amount
Acetone	20mM	10mL
4mM DTT		50µL

Bradford protein assay

Table 4: Preparation of DIGE-buffer

Component	Final concentration	Amount
Urea	7M	21.02g
Thiourea	2M	7.61g
→ *dissolved in ddH_2O*		
Amberlite IRN-150L	1%	0.375g
→ *stirred for 1 hour* → *filtered (0.2µm)*		
Tris	15nM	0.0908g
→ *pH ≥ 8.5*		
CHAPS	4%	2.0g
→ *filtered (0.2µm)*		
ddH_2O		added to 50mL
➢ DIGE buffer was aliquoted and stored at -20°C		

2.2.2 Blood collection

Blood was collected in three vacutainer 9mL tubes containing 3.8% sodium citrate, as an anticoagulant. The whole blood tubes were centrifuged for 20min at 120xg at room temperature without deceleration to separate whole blood components. The yellow supernatant represents the PRP, the white band contains the leukocytes and at the bottom of the tube are the erythrocytes. After separation only the upper 2/3 of the PRP were removed (~ 3mL) to prevent any contamination with leukocytes.

2.2.3 Platelet gel filtration and precipitation with TCA

To separate platelets from plasma proteins gel-filtration was performed, which is a type of size-exclusion chromatography. The molecules are separated by their size, in some cases also by their molecular mass. In this case, the stationary phase is the Sepharose-2B column and the mobile phase is a combination of 1xDPBS and PRP. The bigger platelets elute faster than the smaller plasma proteins, which remain in the pores of Sepharose-2B. This method is known to be a very gentle and efficient way to separate the plasma from the platelets [51, 52]. For each sample, two columns were prepared.

Each column was processed as follows:

- Open the outlet of the column and close them with the yellow lid, to keep 1xDPBS and Sepharose-2B in the column.
- Gently pour 1mL 1xDPBS in the column and avoid bubble formation.
- Sepharose-2B is stored in 20% ethanol and should be homogenized thoroughly by mixing before use.
- Gently pour 19mL Sepharose-2B into the column. If there is bubble formation, remove them by gently tapping.
- Add 1xDPBS until it reaches the top of the column and open the column by removing the yellow lid.
- Keep filling the column with 1xDPBS about 20min, until Sepharose-2B sediment reaches between 11-12 mL.
- Soak the frit with enough 1xDPBS, then put the frit horizontally in the column and place it on the top of the Sepharose-2B bed (Sepharose-2B should never run out of 1xDPBS).
- Continue pouring 1xDPBS for 20min.
- Before loading PRP be sure that no 1xDPBS is left in the column.
- Load 1mL PRP in the column.
- Wait till PRP is soaked into Sepharose-2B and then add 2.5mL 1xDPBS.
- Add another 1.5mL 1xDPBS (After this volume the drops should be cloudy).
- Catch the cloudy white drops in a 1.5ml Eppendorf tube.
- Pool the GFP and measure their platelet count using the Haematology cell counter.
- Add 250µL TCA /dithiothreitol solution (80mM DTT) (Table 2) to the 750µL platelet suspension.
- Incubate for one hour at 4°C in the dark, then centrifuge for 10min at 20627xg at 4°C.
- Wash the pellet three times with 1mL cold acetone/DTT solution (20mM DTT) (Table 3).
- Between each wash step, centrifuge for 10min at 20627xg at 4°C.
- Store the pellet in acetone/DTT solution at -80°C.

2.2.4 Bradford protein assay

The Bradford protein assay was used to measure the concentration of total protein in a sample. It is one of the most common colorimetric assay methods for the determination of protein concentration. Coomasie Brilliant Blue G-250 binds to the protein and causes a shift in the absorption maximum from 465 to 595nm. The increase in absorption at 595nm can be detected and is proportional to the protein concentration. Through the comparison of the colour response of the dilution series of BSA with the colour response of the sample, the final concentration of the protein can be determined [53]. In acetone/DTT stored GFP pellets were centrifuged for 10min at 20627xg at 4°C and then the supernatant was carefully removed. The pellets were washed with 1mL cold acetone (-20°C) and centrifuged at the same conditions as before. Again, the supernatant was removed, the pellet was air-dried for 20min and resolubilized in DIGE buffer (Table 4) by shaking overnight at 800rpm at 4°C. The volume of the DIGE buffer was calculated from the formula below:

$$V(\text{DIGE buffer}) = \frac{\text{GFP platelet count} * 1.33 * 0.5}{2.5}$$

Formula 1: Calculation for the volume of DIGE-buffer

1.33= constant

0.5= GFP volume

2.5= requested protein concentration (based on experienced values 2-4µg/µL)

Before measuring the protein concentration, a standard dilution series of BSA was prepared. The standards are necessary to determine in what range the protein concentrations are located.

Table 5: BSA standard dilution series. Aliquoted pro 95µL and stored at -20°C.

	concentration [mg/mL]	**µL BSA [2mg/mL]**	**µL 1xDPBS**
S1	0	0	1615
S2	0.05	42.5	1572.5
S3	0.10	85	1530
S4	0.15	127.5	1487.5
S5	0.20	170	1445
S6	0.25	212.5	1402.5
S7	0.3	255	1360

The samples and standards were diluted 1:20. Samples were diluted in 1xDPBS and the standards in DIGE buffer. 20µL of each standard dilution and samples were applied in triplicates on a 96-well microtiter plate and 200µL of Coomassie Plus Protein Assay Reagent solution was added to each well and incubated for 3min at room temperature in the dark. The plate was then measured at a wavelength of 595nm with an ELISA reader.

An illustrative example of a standard curve is shown in Figure 5:

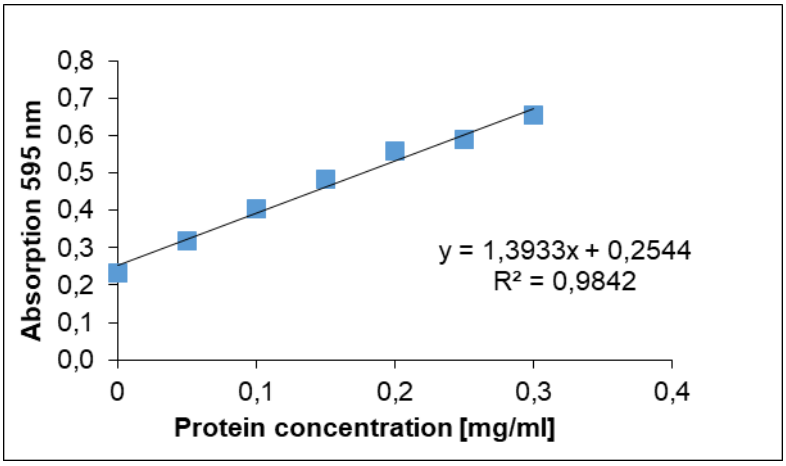

Figure 5: Absorption curve of BSA standard dilutions at 595nm. The sum of the squared residuals (R^2) value of 0.9842 demonstrates the portion of sample variability which is elucidated by the valuation model. In this example, the slope of the straight is 1.3933 and the intercept has a value of 0.2544.

After the measurement of the protein concentration, the samples were aliquoted to 15µg protein amounts and stored at -80°C.

Preparation of Internal Standard

The Internal standard (IS) is used as a necessary tool to minimize technical variance in sample analysis. Ideally, IS should contain the same amount of each sample, which represents the average platelet proteome from AD, MCI and matched controls. The addition of this Cy2-labeled IS in every 2D-DIGE gel of this AD proteomics study, permits a precise detection of small differences in protein levels between samples which means a higher accuracy in protein quantification between samples from different gels. The concentration of the IS was also measured with the Bradford protein assay, aliquoted to 15µg protein amounts and stored at -80°C.

2.3 2D-DIGE

2D-DIGE is an important tool for comparative proteomics, which permits the visualization of thousands of proteins and protein species. This technique allows for the protein separation of three samples in the same gel, this enables the comparison of individual proteins between the different samples to detect changes in abundance. This allows for the characterization of protein markers that depict a specific pathological or physiological state of a cell or tissue. In the application of 2D-DIGE, two different samples and one IS are labelled with a spectrally resolvable fluorescent dye and then separated by their isoelectric point (pI) and molecular mass [54]. After the second dimension, the separated samples were visualized by scanning the gel with the respective excitation wavelength of each dye. Then gel analysis was performed with the DeCyder™ 2D Software. The workflow of 2D-DIGE is shown in Figure 6.

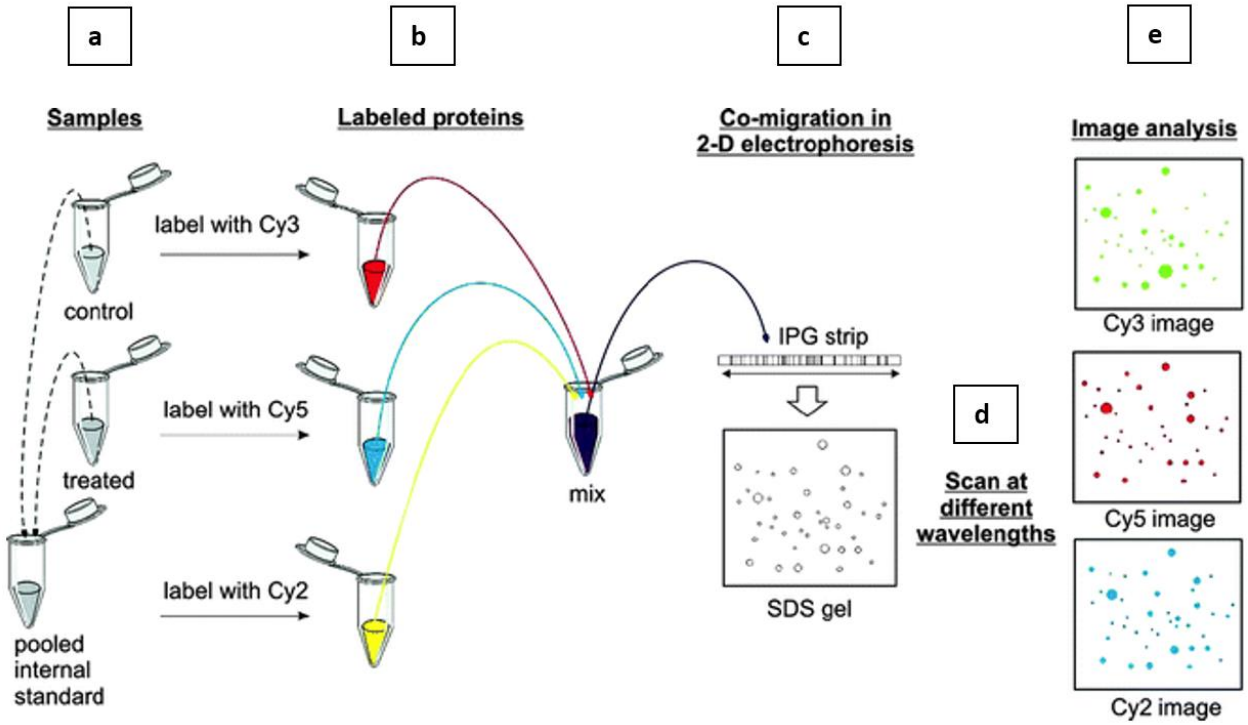

Figure 6: Workflow of the 2D-DIGE method: a) labelling the samples with fluorescent CyDye. b) The first dimension, separating the proteins by isoelectric point. c) The second dimension, separating the proteins by molecular weight in 11.5% acrylamide gels. d) Imaging by scanning at different wavelengths. e) Image analysis via DeCyder™ 2D software. **Figure minimally adapted from source:** Beckett P. (2012) The Basics of 2D DIGE. In: Cramer R., Westermeier R. (eds) Difference Gel Electrophoresis (DIGE). Methods in Molecular Biology (Methods and Protocols), vol 854. Humana Press. [55]

2.3.1 Materials and Solutions

Materials:

DTT (Sigma-Aldrich, #11583786001)

1-Butanol (Merck, #101990)

Acrylamide (Gerbu, #1001)

Agarose (Sigma, #A9539)

Amersham CyDye DIGE Fluors (GE Healthcare, #25-8010-65)

Ammonium persulfate (APS) (Merck, #101201)

Ampholyte pH 4-7 (Serva, #4294801)

Ampholyte pH 6-9 (GE Healthcare, #17600178)

Bis-acrylamide (GE Healthcare, #17130402)

Bromophenol Blue (GE Healthcare, #17-1329)

Dimethylformamide (DMF, 99.8 %) (Sigma-Aldrich, #227056)

Ettan DALTsix (GE Healthcare)

Glycerol (Sigma, #G5516)

Glycine (Merck, #104201)

Hydrochloric acid (HCl) (Merck, #100317)

Immobilized pH gradient strip (IPG, pH 4-7, 24 cm, GE Healthcare, #17-6002-46)

Immobilized pH gradient strip (IPG, pH 6-9, 24 cm, GE Healthcare, #17-6002-47)

Iodoacetamide (IAA) (Sigma-Aldrich, #I1149)

IPGphor (GE Healthcare)

L-Lysine monohydrochloride (Sigma-Aldrich, #L5626)

Sodium dodecyl sulfate-polyacrylamide (SDS) (Biorad, #1610302)

Tetramethylethylendiamine (TEMED, 99 %) (Roth, #T8133)

Typhoon Scanner (Amersham Biosciences)

First dimension solutions:

Table 6: Preparation of CyDye stock solution

Component	Final concentration	Amount
CyDye	5nM	5nM of CyDye powder dissolved in 5.1µL DMF
DMF		
➢ stored at -20 °C		

Table 7: Preparation of CyDye work solution

Component	Amount
CyDye-stock solution (Cy2/Cy3/Cy5)	0.35µL
DMF	2.75µL

Table 8: Preparation of Lysine stock solution

Component	Final concentration	Amount
Lysine	10mM	0.1827g
ddH_2O		added to 100mL
➢ 10 µL aliquots of lysine stored at -80 °C		

Table 9: Preparation of rehydration buffer

Component	Final concentration	Amount
Urea	7M	21.02g
Thiourea	2M	7.61g
→ *dissolved in ddH_2O*		
Amberlite IRN-150L	1%	0.375g
→ *stirred for 1 hour* → *filtered (0.2 µm)*		
CHAPS	4%	2g
→ *filtered (0.2 µm)*		
ddH_2O		added to 50mL
→ *some crumbs of bromophenol blue were added* → *filtered (0.2 µm)*		

Table 10: Preparation of the samples for the IEF pH 4-7

Component	Final concentration	Amount
Labelled protein	12µg/ 150µL	xµL
Rehydration buffer		150µL – xµL
➢ labelled protein samples of patients, controls, and IS were pooled		
Ampholyte (pH 4-7)	1%	4.5µL
4M DTT	70mM	7.9µL

Table 11: Preparation of loading buffer pH 4-7

Component	Concentration	Volume for 6 Strip
Rehydration buffer		450µL
DTT	70mM	7.9µL
Ampholyte solution (pH 4-7)	1%	4.5µL

Table 12: Preparation of the samples for the IEF pH 6-9

Component	Final concentration	Amount
Labelled protein	12µg	x µL
➢ labelled protein samples of patients, control, and IS were pooled		
Rehydration buffer		55µL – x µL of Pool
Ampholyte solution (pH 6-9)	1%	1µL
4M DTT	150mM	2µL

Table 13: Preparation of rehydration mix pH 6-9

Component	Concentration	Volume for 2 Strips
Rehydration buffer		466.5µL
DTT (4mM)	150mM	18.7µL
2% Ampholyte (pH 6-11)	1%	9.9µL

<u>Second dimension solutions:</u>

Table 14: Preparation of agarose solution

Component	Final concentration	Amount
Agarose	0.5%	0.3g
SDS	1.0%	0.6g
Tris solution	375mM	15mL
ddH_2O		added to 60mL
➢ *some crumbs of bromophenol blue were added*		

Table 15: Preparation of 4x LTB buffer

Component	Final concentration	Amount
Tris base	1.5M	22.71g
➢ *pH fitted to 8.68 with HCl at 24°C*		
ddH_2O		added to 125mL

Table 16: Preparation of acrylamide solution

Component	Final concentration	Amount
Acrylamide	29.2%	56.55g
Bis-acrylamide	0.8%	1.54g
➢ *filled up to 100mL and stirred for 1 hour*		
ddH_2O		added to 193mL

Table 17: Preparation of 10x SDS electrophoresis running buffer

Component	Final concentration	Amount
Tris base	250mM	18.15g
Glycine	1.92M	86.46g
ddH_2O		added to 600mL
➢ *11g SDS added freshly before every experiment*		

Table 18: Preparation of saturated 1-butanol solution

Component	Amount
1-Butanol	150mL
ddH_2O	30mL

Table 19: Preparation of polyacrylamide gels (24 cm)

Component	Final concentration	The amount for 6 gels
Acrylamide solution (30%)	11.5%	193mL
4x LTB (1.5M, pH 8.68)	375mM	125mL
ddH_2O		178mL
SDS	0.08%	0.4g
➢ *filtered and degassed for 1 hour*		
APS (10%)	0.08%	3.75mL
TEMED	0.03%	165µL
➢ *stirred gently!*		

Table 20: Preparation of equilibration buffer

Component	Final concentration	Amount
Tris base (pH 8.68)	50mM	15.00mL
Urea	6M	108.11g
Glycerol	30%	103.50mL
SDS	2%	6.00g
ddH_2O		added to 300mL

Table 21: Preparation of DTT-equilibration solution

Component	Final concentration	Amount
DTT	1%	0.250g
Equilibration buffer	filled up with 25mL equilibration buffer	

Table 22: Preparation of IAA-equilibration solution

Component	Final concentration	Amount
IAA	2.5%	0.625g
Equilibration buffer	filled up with 25mL equilibration buffer	

2.3.2 First dimension: Isoelectric focusing (IEF)

IEF procedure for pH 4-7

Each sample was labelled with 0.35µL CyDye (Table 7) and incubated on ice for 35min in the dark. After incubation, the labelling process was stopped by adding 0.5µL Lysine (Table 8) and incubating again for 10min in the dark. Then each sample was filled up to 150µL with Rehydration buffer (Table 9). Afterwards, the patient, control and IS samples were pooled with a total volume of 450µL. Subsequently, 7.9µL DTT (70mM) and 4.5µL 1% Ampholyte (pH 4-7) was added to the samples (Table 10), then centrifuged for 10min at 20627xg at 4°C. After centrifugation, the sample-rehydration solution was transferred into an IPG strip holder, the strips were then placed with the gel side downwards in the sample-rehydration solution. Subsequently, 3mL cover fluid was added to the strip for preventing the strip to dry out (urea buffer crystallizes quickly). The strips were rehydrated for 11 hours. After strip rehydration and before starting the IEF, small filter pads were soaked with loading buffer (Table 11) and placed on the electrodes. Then the strips were placed with the gel side downwards onto the IPG instrument and covered with 5mL cover fluid. Subsequently, IEF was started under the following conditions, shown in Table 23.

Table 23: IEF parameters for IEF pH 4-7. 24cm strips 50uA/strip at 20°C.

Step	Gradient	Voltage [V]	Time [h]
1	Step-n-Hold	200	00:01
2	Step-n-Hold	10	00:01
3	Gradient	200	02:00
4	Step-n-Hold	200	02:00
5	Step-n-Hold	300	02:15
6	Gradient	5000	07:30
7	Step-n-Hold	5000	02:20
8 (safety step)	Step-n-Hold	500	03:00

After IEF, the strips were stored at -80°C until the second dimension was performed.

IEF procedure for pH 6-9

450µL of the rehydration mix (Table 13) was given into the strip holder, then the strip was placed with the gel site downwards in the rehydration mix and covered with 2mL cover fluid. The strip rehydrated for 11 hours. For the sample application, the rehydrated strip was placed with the gel layer upwards into a strip-holder and covered with 5mL cover fluid. Subsequently, filter pads were placed onto the electrodes of the strips. A square-shaped filter pad was placed on the anode side (+), soaked with Rehydration buffer (Table 9) and a rectangle-shaped filter pad, soaked with 175µL cathode loading buffer (Table 13) was placed on the cathode side (-), then the electrodes were positioned on the top of each filter pad. For transferring the sample onto the strip, a cup was placed next to the anode. Sample preparation was performed the same as for pH 4-7. After stopping the labelling reaction with Lysine the samples were pooled (patient, control and internal standard) and Rehydration buffer was added to the samples (total volume 55µL). Subsequently, 2µL DTT (150mM) and 1µL 1% Ampholyte (pH 6-11) were added to the sample (Table 12) and centrifuged for 10min at 20627xg at 4°C. The loading cup was filled with 175µL cover fluid and 55µL of the sample mix. After sample loading, the IPG instrument was started under the following conditions, shown in Table 24.

Table 24: IEF parameters for isoelectric focussing pH 6-9. 24cm strips 50uA/strip at 20°C.

Step	Gradient	Voltage [V]	Time [h]
1	Step-n-Hold	300	00:05
2	Gradient	10	00:01
3	Gradient	300	03:00
4	Gradient	800	05:00
5	Gradient	1400	04:00
6	Step-n-Hold	1400	05:00
7	Gradient	3500	03:00
8	Step-n-Hold	3500	01:00
9 (safety step)	Step-n-Hold	500	04:00

After IEF, the strips were stored at -80°C until the second dimension was performed.

2.3.3 Second dimension: SDS-PAGE

The polyacrylamide gel solution was filled into the gel casting system immediately after preparation (Table 19). After gel casting, 2mL of water-saturated 1-butanol (Table 18) was added to flatten the gels and to prevent dehydration. The gels were left to polymerize for 90min. In the meantime, running buffer (Table 17) was prepared and poured into the chamber. After the polymerization step, the gel plates were taken out of the gel casting system and washed twice with running buffer. This step is necessary for removing 1-butanol. To prevent the gel-surface from drying out, 2mL running buffer was added for each gel. Afterwards, the strips were equilibrated by laying them in the DTT/equilibration solution for 20min (Table 21) and then transferring them into IAA/equilibration solution for 15min (Table 22). After equilibration, the running buffer was poured out from the gels and the strips were transferred on top of the gel front, then covered with 1.8mL agarose solution (Table 14). Bubbles were removed carefully with a spatula. Subsequently, the gels plates were transferred into the running chamber and the program below was applied for the electrophoretic separation of the proteins.

Table 25: Electrophoresis conditions of 24cm polyacrylamide gels.

Step	Voltage (V)	Time (h)
S1	30	1.5
S2	50	3
S3	110	14
manual	210	2

2.3.4 2D-DIGE Scanning and gel analysis with DeCyder™ 2D Software

2D-DIGE Scanning

After SDS-PAGE the gels were scanned in situ with the glass plates using a Typhoon 9410 Scanner (GE Life Science) to visualize the separated proteins in the gel using the following settings, shown in Table 26.

Table 26: Settings of Typhoon laser scanner

Fluorescence	PMT (Photomultiplier)	Excitation	Emission BP-Band pass filter
Cy2 (blue)	530	488 nm	520 nm BP40
Cy3 (green)	575	532 nm	580 nm BP30
Cy5 (red)	550	633 nm	670 nm BP30

Gel analysis with DeCyder™ 2D Software

DeCyder™ 2D Software was implemented to perform spot detection, quantitation and matching according to the study design [56]. At first, spots were detected by DIA (Differential In-gel Analysis) software module. The DIA module enables spot co-detection and image analysis between samples within the same gel. Furthermore, it allows for the detection and the cleaning of spot artefacts by using pre-set filters [56, 57]. To prepare the gels for further analysis, pre-set filters were applied:

- Target spot number was set to 10.000
- Saturated spots with a peak hight above 65.000 were excluded
- Spots with a greater slope than 1.4 were excluded
- Spots with a volume below 25.000 were excluded
- Background of the fluorescent signal of the spots was corrected for and normalized

The Biological Variation Analysis (BVA) module was used for pairwise image analysis among multiple gels. The ratios of differences in protein abundance were depicted as fold changes between patients and controls [56]. The gels were transferred from DIA to the DeCyder™ module BVA where the gels were classified in the following categories: MCI male-, MCI female-, MCI control male-, MCI control female-, AD male-, AD female-, AD control male- and AD control female-folder. The gels were manually matched (250-350 spots) and then the automatic match was applied to detect more spots. On average 4100 spots were found by the automatic match. The standard abundance of each protein spot was calculated by dividing the spot volume through the corresponding spot volume of the IS. As a result, differences in the protein abundance within and between gels could be detected. A preliminary

statistical analysis was performed using DeCyder™ software (version 7.0). The statistical significance for each group (male AD/Co, male MCI/Co, female AD/Co and female MCI/Co) was calculated using a t-Test. Only proteins that matched in 80% of all 2D-DIGE gels and displayed an average ratio of ± 12% and a p-value of < 0.05 were considered as relevantly altered. These proteins were selected for the MS identification.

2.4 Silver staining – compatible for MS

Silver staining is a common method to detect proteins after electrophoretic separation on polyacrylamide gels. This method has several advantages such as high sensitivity, simple to use and cheap chemicals. Another benefit is the stability of silver-stained proteins, lasting for several weeks. Furthermore, silver staining is compatible with MS analysis after trypsin digestion [58].

2.4.1 Materials and Solutions

Materials:

Acetic acid (CH_3COOH, 100%) (Merck, #100063)
Silver nitrate ($AgNO_3$) (Fluka, #319449)
Sodium carbonate (Na_2CO_3) (Merck, #106392)
Formaldehyde (37%) (Merck, #104003)
Sodium thiosulfate pentahydrate ($Na_2S_2O_3 * 5H_2O$) (Merck, #106516)

Solutions:

Table 27: Preparation of fixing solution

Component	Final concentration	Amount
Ethanol	50%	500mL
Acetic acid	5%	50mL
ddH_2O	45%	450mL

Table 28: Preparation of washing solution

Component	Final concentration	Amount
Ethanol	50%	500mL
ddH_2O	50%	500mL

Table 29: Preparation of sensitizing solution

Component	Final concentration	Amount
Sodium thiosulfate pentahydrate	0.025%	0.25g
ddH_2O		added to 1000mL

Table 30: Preparation of silver solution

Component	Final concentration	Amount
Silver nitrate	0.15%	8.8mL
ddH_2O		added to 1000mL

Table 31: Preparation of developing solution

Component	Final concentration	Amount
Formaldehyde	0.04%	0.4mL
Sodium carbonate	2%	20g
ddH_2O		added to 1000mL

Table 32: Preparation of stop solution

Component	Final concentration	Amount
Acetic acid	5%	50mL
ddH_2O		added to 1000mL

Table 33: Preparation of storage solution

Component	Final concentration	Amount
Acetic acid	1%	10mL
ddH_2O		added to 1000mL

2.4.2 Silver staining of the proteins

The sequential phases of silver staining are as described below:

- Protein fixation with fixing solution
- Protein washing with washing solution
- Protein washing with ddH_2O
- Protein sensitizing with sensitizing solution
- Protein washing with ddH_2O
- Protein silver impregnation with silver solution
- Protein washing with ddH_2O
- Image development with developing solution
- Terminating the staining process with stopping solution
- Storage in 1% Acetic acid

After electrophoresis, the gels were taken out of the glass plates and incubated on a shaker for 20min in fixing solution (Table 27). After fixing the protein by blocking the proteins to diffuse further in the gel, the gels were washed with a washing solution for 10min (Table 28). Thereafter the gels were washed with ddH_2O for 2hours via shaking. Subsequently, the gels were incubated with sensitizing solution for 3min (Table 29) and washed twice with ddH_2O for 1min. After washing, the gels were incubated for 45min via shaking in silver solution (Table 30). To diminish the background of silver staining the gels were washed twice with ddH_2O for 1min. Then the gels were incubated in developing solution until the desired intensity of the protein spots was achieved (Table 31). The image development was terminated by adding the stop solution for 5min (Table 32). This stopping step was repeated a total of three times. Finally, the gels were stored in the storage solution (Table 33) overnight at 4°C.

2.5 Trypsin digestion for MS

2.5.1 Materials and Solutions

Materials:

Ammoniumhydrogencarbonate (NH_4HCO_3) (Applichem, #A3583)

Potassium hexacyanoferrate (III) ($K_3Fe(CN)_6$) (Sigma-Aldrich, #31253)

Sodium thiosulfate pentahydrate ($Na_2S_2O_3$ * $5H_2O$) (Merck, #106516)

Trypsin (Promega, #V511A)

Stock solutions:

Table 34: Preparation of de-staining stock solution

Component	Final concentration	Amount
10x Potassium hexacyanoferrate(III)	150mM	0.4938g
10x Sodium thiosulfate pentahydrate	500mM	1.2409g
ddH_2O		added to 10mL

Table 35: Preparation of DTT protein modifying stock solution

Component	Final concentration	Amount
DTT (100x)	1M	1.5425g
ddH_2O		added to 10mL

Table 36: Preparation of IAA protein modifying stock solution

Component	Final concentration	Amount
IAA (10x)	500mM	0.9248g
ddH_2O		added to 10mL

Table 37: Preparation of trypsin stock solution in 50 mM acetic acid

Component	Final concentration	Amount
Trypsin	8x	20µg
Acetic acid	50mM	200µL
→ dissolved 10min on ice, aliquoted à 10µL and stored at -80°C		

Working solutions:

Table 38: Preparation of de-staining solution

Component	Final concentration	Amount
10x Potassium hexacyano ferrate(III) (150mM)	15mM	3mL
10x Sodium thiosulfate pentahydrate (500mM)	50mM	3mL
ddH_2O		added to 30mL
➢ prepared freshly on the day of usage		

Table 39: Preparation of working solution

Component	Final concentration	Amount
Ethanol (100%)	50%	60mL
Acetic acid (100%)	10%	12mL
ddH_2O		added to 120mL
➢ prepared freshly on the day of usage		

Table 40: Preparation of ammoniumhydrogencarbonate solution

Component	Final concentration	Amount
Ammoniumhydrogencarbonate	50mM	0.593g
ddH_2O		added to 150mL
➢ prepared freshly on the day of usage		

Table 41: Preparation of reducing agent

Component	Final concentration	Amount
Ammoniumhydrogencarbonate-solution (50mM)		29.70mL
DTT (100x)	10mM	300µL
➢ prepared freshly on the day of usage		

Table 42: Preparation of alkylating agent

Component	Final concentration	Amount
Ammoniumhydrogencarbonate-solution (50mM)		27mL
10x IAA	50mM	3mL
➢ prepared freshly on the day of usage		

Table 43: Preparation of 1x trypsin

Component	Final concentration	Amount
Trypsin (8x)	1x	50µL
Ammoniumhydrogencarbonate-solution (50mM)		added to 400µL
➢ prepared freshly on the day of usage		

Table 44: Preparation of elution buffer

Component	Final concentration	Amount
Acetonitrile (100%)	50%	2.5mL
Formic acid (96%)	5%	250µL
ddH_2O		2.25mL
➢ prepared freshly on the day of usage		

2.5.2 Trypsin digestion

After silver staining, photos of the polyacrylamide gels were taken before and after cutting out the spots to document the position of each protein spot of interest. Afterwards, the spots were washed three times in an Eppendorf tube with 500µL 1% acetic acid for 3min, then they were de-stained with 500µL de-staining solution for 2 – 3min (Table 38). To remove the de-staining solution the spots were incubated with 500µL working-solution (Table 39) on a thermoblock four times, twice for 5min and twice for 10min. To regulate the right pH, the spots were washed with 500µL ammoniumhydrogencarbonate-buffer (Table 40) for 5min. Subsequently, the spots were incubated with ammoniumhydrogencarbonate and DTT (Table 41) for 30min at 56°C to reduce the disulfide bonds. Then washed in 500µL ammoniumhydrogencarbonate for 5min. To alkylate the already disrupted disulfide bonds, the spots were incubated in ammoniumhydrogencarbonate and IAA (Table 42) for 20min at room temperature in the dark. Afterwards, another washing step with 500µL ammoniumhydrogencarbonate followed. Then the spots were incubated with 100 – 150µL acetonitrile until the spots had a homogenous white colour. Until this point, the supernatant was discarded before each step. The gel pieces were dried for 20min in the speed vac. After drying the spots were incubated in 10 –15µL 1x trypsin solution (Table 43) for 15min on ice. Subsequently, the spots were added a volume of 10 – 20µL ammoniumhydrogencarbonate-buffer and incubated under soft shaking at 37°C overnight. On the next day, the samples were centrifuged for 1min at 112 x g, then the samples were incubated in 20µL ammoniumhydrogencarbonate-buffer for 30min. Afterwards, the samples were incubated for 15min in an ultrasonic bath and centrifuged for 1 min at 112 x g. The supernatant was transferred into a silicon covered reaction tube and 30µL of the elution buffer (Table 44) was added to the gels. The samples were incubated for 10min in the ultrasonic bath, centrifuged for 1 min at 112 x g and transferred into the silicon covered reaction tube. Once again, 30µL of the elution buffer was added to the gels, incubated for 10min in the ultrasonic bath, centrifuged for 1 min at 112 x g and transferred into the silicon covered reaction tube. The total volume collected from each supernatant of the last three steps was reduced to 25µL in the speed-vac. The samples were either analyzed directly with MS or stored at -80°C until MS analysis.

2.6 Western Blot

Proteomics technologies such as MS or 2D-DIGE are valuable methods to identify highly complex mixtures and comprehensive expression patterns allowing us a better understanding of molecular events. Typically the resulting data are validated by a second independent method such as Western blot. WB has become a common technique globally for immunodetection and quantification of particular proteins [59]. The proteins are separated on a gel by their molecular weight and migrate due to electric currents toward the anode. The transfer from the gel to the nitrocellulose membrane works on the same principle. The protein of interest can be detected by incubating with a specific corresponding primary antibody. The primary antibody can be detected due to the binding of a fluorescence-labelled or with a chemiluminescence-labelled second antibody [60].

2.6.1 Materials and Solutions

Materials:

Blotting Grade Blocker Non-Fat Dry Milk (Biorad, #170-6404)

GDI1 (Biorbyt, #orb167368) Species: Rabbit; Type: Polyclonal

ImageQuant 8.0 (GE Healthcare)

Rabbit IgG (Novus, #NBP1-75634) Species: Rabbit; Conjugate: DyeLight 650

Tris (bathophenanthroline disulfonate) ruthenium (II) sodium salt solution (RuBPS) (Sigma, #03038-50UL-F)

Typhoon FLA 9500 (GE Healthcare)

Solutions:

Table 45: Preparation of 10x running buffer

Component	Final concentration	Amount
Tris base	0.25M	30.28g
Glycine	1.92M	144.12g
ddH_2O		added to 1000mL

Table 46: Preparation of 4x LTB

Component	Final concentration	Amount
Tris base	1.5M	18.17g
➢ *pH adjusted to exactly 8.68 with HCl at 24°C*		
ddH_2O		added to 100mL

Table 47: Preparation of 4x UTB

Component	Final concentration	Amount
Tris base	1.5M	9.09g
➢ *pH adjusted to exactly 6.8 with HCl at 24°C*		
ddH_2O		added to 50mL

Table 48: Preparation of acrylamide solution

Component	Final concentration	Amount
Acrylamide	29.2%	43.80g
Bis-acrylamide	0.8%	1.20g
ddH_2O		added to 150mL
➢ *filtered before use*		

Table 49: Preparation of 5x SLAB buffer

Component	Final concentration	Amount
Tris base	150mM	0.109g
➢ *pH adjusted to exactly 8.68 with HCl at 24°C*		
SDS	7.5%	0.45g
Glycerol (96%)	375%	2.25mL
ddH_2O		added to 6mL

Table 50: Preparation of 11.5% separating gels

Separating gel (7cm, 1.5mm thick)		
Component	**Final concentration**	**Amount for 2 gels [Final: 18mL]**
Acrylamide solution (30%)	11.49%	7.0mL
4x LTB (1.5M, pH 8.68)	375mM	4.5mL
ddH_2O		6.32mL
SDS (10%)	0.10%	180µL
➢ *mixed gently*!		
APS (10%)	0.04%	72µL
TEMED	0.01%	18µL
➢ *mixed gently!*		

Table 51: Preparation of stacking gels

Stacking gel (24cm x 20cm, 1 mm thick)		
Component	**Final concentration**	**The amount for 2 gels [Final: 8mL]**
Acrylamide solution (30%)	4.0%	940µL
4x UTB (1.5M, pH 8.68)	375mM	2.00mL
ddH_2O		4.98mL
SDS (10%)	0.10%	80µL
➢ *mixed gently!*		
APS (10%)	0.04%	32µL
TEMED	0.01%	8µL
➢ *mixed gently!*		

Table 52: Preparation of blotting buffer

Component	Final concentration	The amount for 2 gels
10x Running buffer	1x	130mL
SDS	1.73mM	0.65g
Ethanol (96%)	19.20%	260mL
ddH_2O	0.10%	added to 1300mL

Table 53: Preparation of fixing solution

Component	Final concentration	The amount for 2 gels
Acetic acid (100%)	7%	14mL
Ethanol (96%)	10%	20.8mL
ddH_2O		added to 200mL

Table 54: Preparation of ruthenium stain solution

Component	Final concentration	The amount for 2 gels
Ruthenium stain	1:100,000	1µL
ddH_2O		added to 1000mL

Table 55: Preparation of 5% blocking solution

Component	Final concentration	Amount
non-fat dry milk powder	5%	5g
1x DPBS-Tween-20		added to 100mL

Table 56: List of antibodies used in Western blotting

Primary antibody	**species**	**type**	**dilution**
GDI 1	Rabbit	Polyclonal	1:1250
Secondary antibody	**species**	**conjugate**	**dilution**
Rabbit IgG	Rabbit	DyeLight 650	1:500

2.6.2 1D-WB

Gel casting

After assembling the gel casting apparatus, the separating gel was prepared (Table 50). APS and TEMED were added under gentle mixing just before gel casting. Each gel casting system was filled with 7mL separating gel solution. To prevent the gels from drying out, 1mL of ddH_2O-saturated 1-butanol was added on top of the gels. The gels were left to polymerize for 45min. In the meantime, the stacking gel was prepared (Table 51). After polymerization, the 1-butanol layer was removed by washing with ddH_2O. Immediately after the casting of the slacking solution, a comb with 36-wells was applied on top of the gels and then left to polymerize for 45min. In the meantime, the samples were prepared for electrophoresis.

Sample preparation

The 5x SLAB buffer was previously prepared, aliquoted and stored at -20°C (Table 49). For sample preparation the 5x SLAB-buffer was mixed with 4M DTT (200µL 5x SLAB + 25µL 4M DTT). Subsequently, 13µg of each protein extract was mixed with 5x SLAB buffer and ddH_2O to attain a final concentration of 1x SLAB buffer [0.5M DTT]. The proteins were denaturated by heating the sample-buffer mixture at 95°C for 4min. To get rid of the possible impurity the samples were centrifuged at full speed for 3min

at room temperature. Afterwards, the comb in the stacking gel was carefully removed and the slots were washed with 1x running buffer (Table 45). The exact volume equal to a protein amount of 13µg of a molecular weight standard (1µL/ lane) was pipetted into the gel well. Then, the electrophoresis was performed under the following conditions (Table 57)

Table 57: Running conditions of 1D gel electrophoresis

Voltage [V]	Time [h]
50	00:20
100	02:30

Blotting procedure

After protein separation by gel electrophoresis, the proteins were transferred from the gel onto a nitrocellulose membrane by WB. Before assembling a gel-membrane sandwich, the blotting buffer was prepared (Table 52). A tray was filled with blotting buffer and the sandwich was consolidated within a gel-holder-cassette as showed in Figure 7.

Figure 7: Exemplary picture for western blot wet transfer sandwich. A foam pad and four Whatman-chromatography papers (20x 15cm) and the polyacrylamide gel were positioned on the cathode (-) side. Directly under the polyacrylamide gel, a nitrocellulose membrane (13x 8cm) was positioned followed by four Whatman-chromatography papers (20x 15cm) and a second foam pad. All components were pre-soaked in blotting buffer. Under the electric current, the proteins migrate from the cathode (gel) to the anode (nitrocellulose membrane). **Source:** https://www.sinobiological.com/category/wb-wet-transfer, accessed on 16th April 2020.

Subsequently, the gel-cassette was positioned into the buffer-tank filled with blotting buffer. Blotting was performed under the following conditions:

Table 58: Blotting conditions of 1D gel electrophoresis, 4 °C

Voltage [V]	Time [h]
50	00:30
75	02:00

After the blotting procedure, the nitrocellulose membrane was washed three times for 5min with 1x DPBS-Tween-20 (0.3%).

Ruthenium stain

To determine the protein quantity the nitrocellulose membrane was stained with ruthenium. First, the nitrocellulose membrane was incubated with a fixing solution (Table 53) for 15min at room temperature. To remove the fixing solution, the nitrocellulose membrane was washed three times for 5min with ddH_2O. Afterwards, the nitrocellulose membrane was incubated overnight at 4°C under gentle shaking with ruthenium solution (Table 54). On the next day, the nitrocellulose membrane was washed three times for 5min with ddH_2O to remove the ruthenium staining solution. Then washed again for three hours with ddH_2O via shaking at 4 °C. Subsequently, the membrane was scanned using Typhoon FLA 9500 scanner. After scanning, the nitrocellulose membrane was washed for 5min with ddH_2O, then transferred into a 5% blocking solution (Table 55) and blocked by shaking overnight at 4° C.

Antibody incubation

The overnight blocked WB membranes were washed three times with 1x DPBS-Tween-20 (0.3%) for 5min. The primary antibody (Table 56) was diluted in 3% milk in 1x DPBS-Tween-20 (0.3%) and then incubated with the nitrocellulose membrane for 2 hours at room temperature via shaking at 180 rpm. After the incubation, the nitrocellulose membrane was washed again three times with 1x DPBS-Tween-20 (0.3%) for 5min. Afterwards, the secondary antibody (Table 56) was diluted in 3% milk in 1x DPBS-Tween-20 (0.3%) and then incubated with nitrocellulose membranes for 1.5 hours at room temperature via shaking at 65 rpm. Again, the nitrocellulose membrane was washed two times in 1x DPBS-Tween-20 (0.3%) for 5min. The third and last time the nitrocellulose membrane was washed with 1x DPBS for 5min.

Antibody detection

The membrane was scanned using a Typhoon laser scanner. To check if the lasers were working and to adjust the PMT voltage parameters, a pre-scan was performed. Then the signal was detected by scanning the corresponding CyDye wavelength, as depicted in Table 59.

Table 59: Settings of Typhoon laser scanner

Fluorescence	PMT	Excitation	Emission BP-Band pass filter
Cy5 – red	560	633 nm	670 nm BP30
Cy2 – blue	560	488 nm	520 nm BP40
Cy3 – green	560	532 nm	580 nm BP30

2.6.3 2D-WB

Two-dimensional Western blot was performed to reconfirm the already identified proteoforms by MS. For the 2D Western blot, the same procedure was used as described in chapter 2.3 (IEF for pH 4-7) except for a different labelling procedure. An amount of 36µg platelet protein sample was labelled with 0.35µL Cy2 working solution. The labelled sample was incubated for 35min on ice in the dark, after which the labelling reaction was stopped using 0.5µL Lysine. Subsequently, the labelled sample was mixed with rehydration buffer. After the gel electrophoresis, the region of interest was cut out and blotted onto a nitrocellulose membrane, as described in chapter 2.6.2 (Blotting procedure). The 2D-WB blotting conditions are shown in Table 60.

Table 60: Blotting conditions of 2D-WB, 4 °C

Voltage [V]	Time [h]
75	90

After blotting, the nitrocellulose membrane was scanned between 500-900 PTM by using a Typhoon FLA 9500 scanner. In this case, ruthenium staining was not performed. The nitrocellulose membrane was incubated with primary and secondary antibody similarly to the 1D-WB (Antibody incubation) and the signal was detected to the corresponding wavelength (Table 59) by using a Typhoon FLA 9500 scanner.

2.6.4 Statistics

Statistical analysis was performed using DeCyder™ software (version 7.0) for the pH range 6-9 and SPSS (Statistical Package for Social Sciences, version 17.0.2.) for the pH range 4-7. The following inclusion criteria were applied to identify biomarker candidates: proteins that had been matched in 80% of all 2D-DIGE gels, displayed a minimum average ratio of ± 12% and a p-value of < 0.05. The differences in protein standardized abundance (SA) between sex divided cognitive impaired (MCI, AD) and healthy controls were reported as an average standardized abundance ratio. The statistical significance within each of the groups was calculated by a Student´s t-Test. For the pH range 4-7, a normality test was calculated with Kurtosis and Skewness. Additionally, the statistical difference between the groups was calculated using a 2-way analysis of variance (2-ANOVA). The Spearman-Rho correlation coefficient was chosen to calculate the correlation between 2D-DIGE and WBs. Graphs were made by GraphPad Prism (version 6.0).

3. Results

This study aimed to elucidate cognitive stage- and sex- differences in Alzheimer's- related platelet protein biomarkers by comparing age- and sex-matched MCI- and AD- patients with healthy controls. Therefore, a comparative proteome analysis (2D-DIGE) was conducted to identify the protein abundance differences between patients and controls.

3.1 Characteristics of study participants

Altogether, we examined 174 cognitive impaireds (CI) patients; 115 AD patients (77 females and 38 males), 59 MCI patients (44 females and 15 males) and 157 healthy controls (101 females and 56 males) in the pH range 4-7. Additionally, 151 cognitive impaireds (CI) patients; 108 AD patients (75 females and 33 males), 43 MCI patients (31 females and 12 males) and 155 healthy controls (101 females and 54 males) were analysed in the pH range 6-9. Within the framework of my master thesis, a total of 36 patients and 36 controls which were pairwise sex- and age-matched (10 AD male patients, 8 MCI male patients, 8 AD female patients, and 10 MCI female patients) were analysed in both pH ranges pH 4-7 and pH 6-9. The rest of the 2D-DIGE data were contributed by the Dr Zellner research group. Details of the study participants and demographics, clinical and laboratory information are shown in Table 61, Table 62 and Table 63.

Table 61: Population demographic, clinical and laboratory data for the study participants in the pH range 4-7.
AD: alzheimer´s disease; MCI: mild cognitive impaired; Co: control; MMSE: mini-mental state examination; APOE: apolipoprotein E.

Characteristics mean	All Patients			Female			Male		
	AD	MCI	Co	AD	MCI	Co	AD	MCI	Co
n	115	59	157	77	44	101	38	15	56
Age (y) ±SD	80.18 ± 6.718	77.31 ± 7.892	78.54 ± 7.383	81.14 ± 6.386	78.32 ± 8.313	79.61 ± 7.626	78.24 ± 7.034	74.33 ± 5.753	76.59 ± 6.547
MMSE ±SD	16.00 ± 7.370	27.59 ± 1.416	28.78 ± 1.136	14.56 ± 7.887	27.43 ± 1.500	28.76 ± 1.181	17.97 ± 6.182	28.07 ± 1.033	28.81 ± 1.076
Education (y)	11.22 ± 3.013	11.60 ± 2.271	12.62 ± 2.939	10.00 ± 2.171	11.60 ± 2.592	11.94 ± 2.634	12.29 ± 3.293	11.60 ± 0.910	13.56 ± 3.107
Laboratory values									
Platelet count [G/L] ±SD	141.89 ± 105.837	135.64 ± 43.318	128.22 ± 59.328	198.67 ± 172.018	130.613 ± 40.636	138.82 ± 73.859	113.50 ± 34.979	150.40 ± 48.879	118.50 ± 43.186
APOE4 (%) heterozygote	47.8	25.4	14	27	20.5	9.9	36.8	40	21.4
APOE4 (%) homozygot	19.1	3.4	0.6	7.2	2.3	1	21.1	6.7	0

Table 62: 2D-DIGE study participants classified by gender, disease stage and controls in the pH range 4-7. CI: cognitive impaired; Co: control; AD: Alzheimer's disease, MCI: mild cognitive impaired

N	All		Female			Male		
	CI	Co	AD	MCI	Co	AD	MCI	Co
	174	157	77	44	101	38	15	56

Table 63: 2D-DIGE study participants classified by gender, disease stage and controls in the pH range 6-9. CI: cognitive impaired; Co: control; AD: alzheimer´s disease, MCI: mild cognitive impaired

N	All		Female			Male		
	CI	Co	AD	MCI	Co	AD	MCI	Co
	151	155	75	31	101	33	12	54

3.2 Identification of sex- and cognitive stage-dependent protein biomarkers in the pH range 4-7

For the identification of sex- and stage-dependent protein biomarkers, the platelet proteome of patients (AD and MCI) were compared to sex- and age-matched controls. Out of 4209 detected protein spots in the pH 4-7, 250-300 were matched manually in each Cy2 labelled 2D-DIGE image. Only proteins which matched in 80% of all 2D-DIGE gel images were statistically evaluated. According to that selection criteria, 649 protein spots were statistically analysed for sex- and stage-dependent abundance changes. Moreover, only proteins with a standardised abundance ratio (Av. Ratio) higher than ± 12% and p-values smaller than < 0.05 were defined as eligible cognition and sex-dependent biomarkers. Fifteen proteins fulfilled these criteria and these proteins were successfully identified by MS. The normality test of the data was calculated with Kurtosis and Skewness. Since the data were normal or nearly normal distributed, the statistical significant cognitive-stage and sex differences between the study groups (male AD/Co, male MCI/Co, female AD/Co and female MCI/Co) were calculated with a 2-way ANOVA. Afterwards, the particular significant differences between the particular study groups pairs were calculated post hoc by a student t-Test. These proteins are depicted in Figure 8. The corresponding statistics of identified proteins are listed in Table 64. An exception was made by alpha-synuclein (Av. Ratio of 1.09) due to its already known link in AD disease [11, 61].

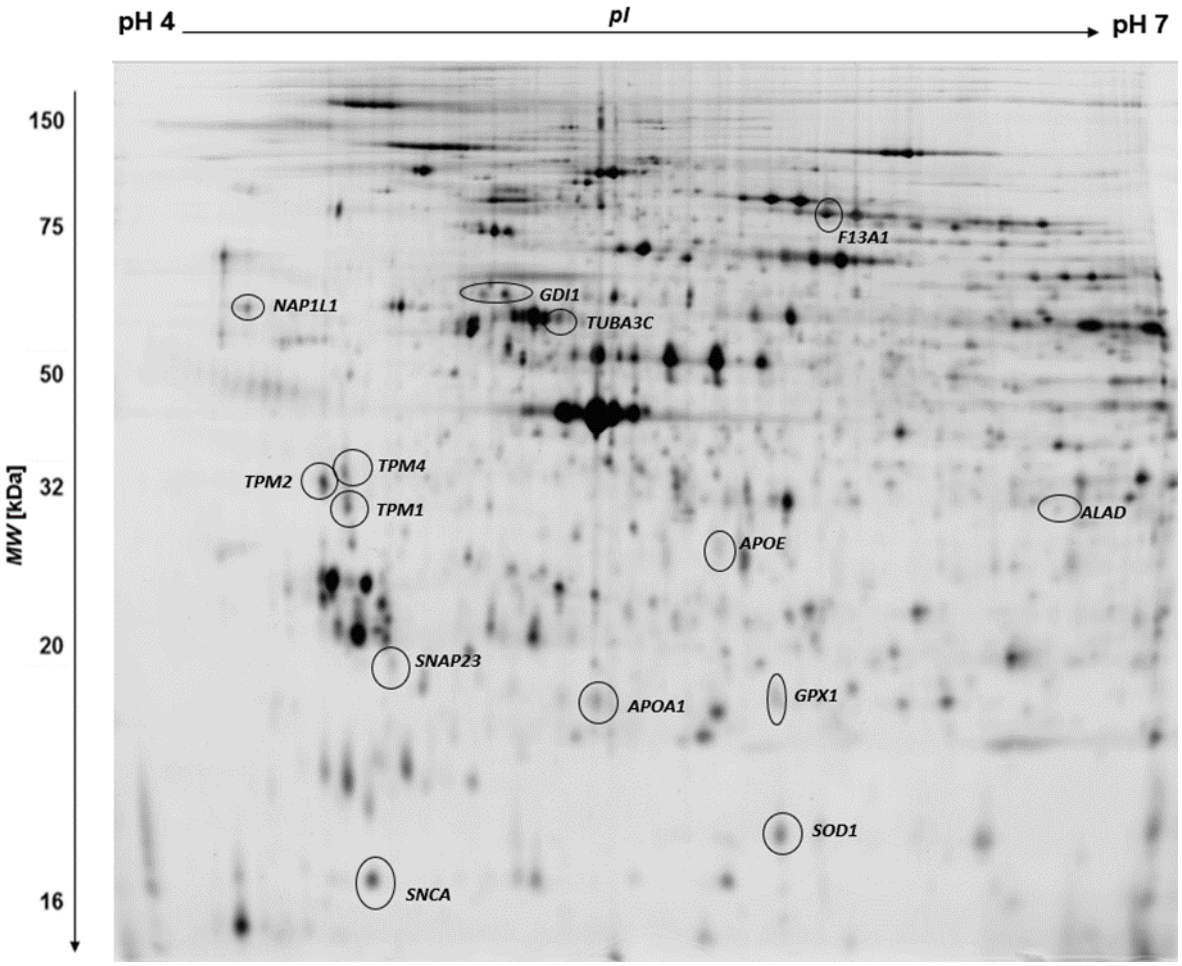

Figure 8: Representative 2D-DIGE gel with highlighted differentially expressed platelet proteins. CyDye-labelled proteins separated according to their molecular weight (MW) and their isoelectric point (pI). Highlighted spots were identified by MS and are shown with their gene name on this gel. Tubulin alpha-3 chain (TUBA3C), Tropomyosin beta chain (TPM2), Tropomyosin alpha-4 chain (TPM4), Tropomyosin alpha-1 chain (TPM1), Apolipoprotein A-I precursor (APOA1), Delta-aminolevulinic acid dehydratase (ALAD), Alpha-Synuclein (SNCA), Rab GDP dissociation inhibitor alpha (GDI1), Glutathione peroxidase 1 (GPX1), Superoxide dismutase 1 (SOD1), Coagulation factor XIII A chain precursor (F13A1), Nucleosome assembly protein 1-like 1 (NAP1L1), Apolipoprotein E3 precursor (APOE), Synaptosomal-associated protein 23 (SNAP23).

Table 64: Potential protein biomarker candidates for AD and MCI patients. Proteome analysis was performed in the pH range 4-7. Proteins of interest were selected according to the following criteria: p-value < 0.05 and proteins which matched in more than 80% of 2D-DIGE gels. The Av. Ratio was calculated by dividing the mean SA of each protein of each sex defined, cognitive impaired group by the corresponding mean SA of the control group. The statistical significance for each group was calculated by a Student´s t-Test using the SPSS Statistics 24 software (p-value < 0.05). Statistical differences between the study groups were analysed using a two-way ANOVA (2-ANOVA), main effects "cognition" and "sex", interaction term "interact". To provide a good overview the p-value of the significant proteins were labelled in different colours: male AD/MCI in blue, female AD/MCI in pink and 2-ANOVA groups (cognition, sex, interact) in orange. N (AD male)= 38, N (MCI male)= 15, N (Co male)= 56, N (AD female)= 77, N (MCI female)= 44, N (Co female)= 101. AD (Alzheimer´s disease), MCI (Mild cognitive impairment), Co (Control).

No.	Uniprot ID	Gene name	Protein Name pH 4-7	2-ANOVA cognition	2-ANOVA sex	2 ANOVA interact	Av. Ratio male AD/Co	p-value male AD/Co	Av. Ratio female AD/Co	p-value female AD/Co	Av. Ratio male MCI/Co	p-value male MCI/Co	Av. Ratio female MCI/Co	p-value female MCI/Co
1	P0DPH7	*TUBA3C*	Tubulin alpha-3 chain	0.003	0.001	0.838	1.03	0.452	0.95	0.040	1.16	0.004	1.03	0.320
2	P07951	*TPM2*	Tropomyosin beta chain	0.809	0.058	0.011	0.95	0.566	1.15	0.026	0.90	0.393	1.23	0.009
3	P02647	*APOA1*	Apolipoprotein A-I precusor	0.443	0.761	0.032	1.39	0.130	0.90	0.424	0.95	0.838	1.68	0.004
4	P13716	*ALAD*	Delta-aminolevulinic acid dehydratase	0.032	0.587	0.591	0.88	0.026	0.92	0.059	0.95	0.599	0.98	0.754
5	P37840	*SNCA*	Alpha-Synuclein	0.321	0.023	0.789	1.09	0.022	1.01	0.745	1.07	0.223	0.99	0.711
6	P31150	*GDI1*	Rab GDP dissociation inhibitor alpha (pI 4.50)	0.022	0.176	0.650	1.23	0.007	1.11	0.043	1.21	0.058	1.09	0.254
7	P31150	*GDI1*	Rab GDP dissociation inhibitor alpha (pI 5.0)	0.009	0.003	0.915	1.10	0.006	1.02	0.365	1.18	0.002	1.08	0.040
8	P07203	*GPX1*	Glutathione peroxidase 1	1.2625E-08	0.929	0.583	0.83	7.1941E-06	0.85	1.7723E-07	1.02	0.753	1.00	0.919
9	P00441	*SOD1*	Superoxide dismutase 1	0.068	0.035	0.495	1.24	0.011	1.04	0.544	1.22	0.085	1.05	0.526
10	P00488	*F13A1*	Coagulation factor XIII A chain precursor	0.052	0.244	0.229	1.00	0.974	1.21	0.004	1.25	0.096	1.15	0.093
11	P55209	*NAP1L1*	Nucleosome assembly protein 1-like 1	0.055	0.008	0.795	1.05	0.167	0.96	0.121	1.12	0.019	1.03	0.377
12	P67936	*TPM4*	Tropomyosin alpha-4 chain	0.640	4.8168E-05	0.012	0.87	0.032	1.08	0.114	0.87	0.177	1.23	9.282E-04
13	P02649	*APOE*	Apolipoprotein E3 precursor	0.009	0.588	0.018	0.90	0.591	0.57	6.225E-05	0.51	0.017	0.88	0.508
14	O00161	*SNAP23*	Synaptosomal-associated protein 23	0.006	0.053	0.812	1.00	0.887	0.96	0.128	1.12	0.019	1.04	0.207
15	P09493	*TPM1*	Tropomyosin alpha-1 chain	0.591	0.036	0.196	0.97	0.715	1.07	0.251	0.96	0.665	1.19	0.013

3.3 Detailed description of selected cognition and sex-dependent platelet biomarkers

Among the fifteen significantly altered proteins, four proteins were selected for detailed investigation in this master thesis. Alpha-synuclein, Rab GDP dissociation inhibitor alpha, Superoxide dismutase 1 and Glutathione peroxidase 1 were chosen due to their already described changes in brains of AD cases [11, 12, 61-67]

3.3.1 Alpha-synuclein is significantly increased in male AD patients

The 2-way ANOVA revealed a cognition stage- independent (p= 0.321) and a sex-dependent (p= 0.023) change of alpha-synuclein (SNCA). This mainly neuronal described protein was significantly increased between AD male and control male (Av. Ratio= 1.09, p= 0.022). The male AD patients show an increase in the protein abundance (+9%) in comparison to matched healthy controls. SNCA were not significantly changed in female AD patients (Av. Ratio= 1.01, p= 0.745), female MCI patients (Av. Ratio= 0.99, p= 0.711) and male MCI patients (Av. Ratio= 1.07, p= 0.223) when compared to their respective control groups.

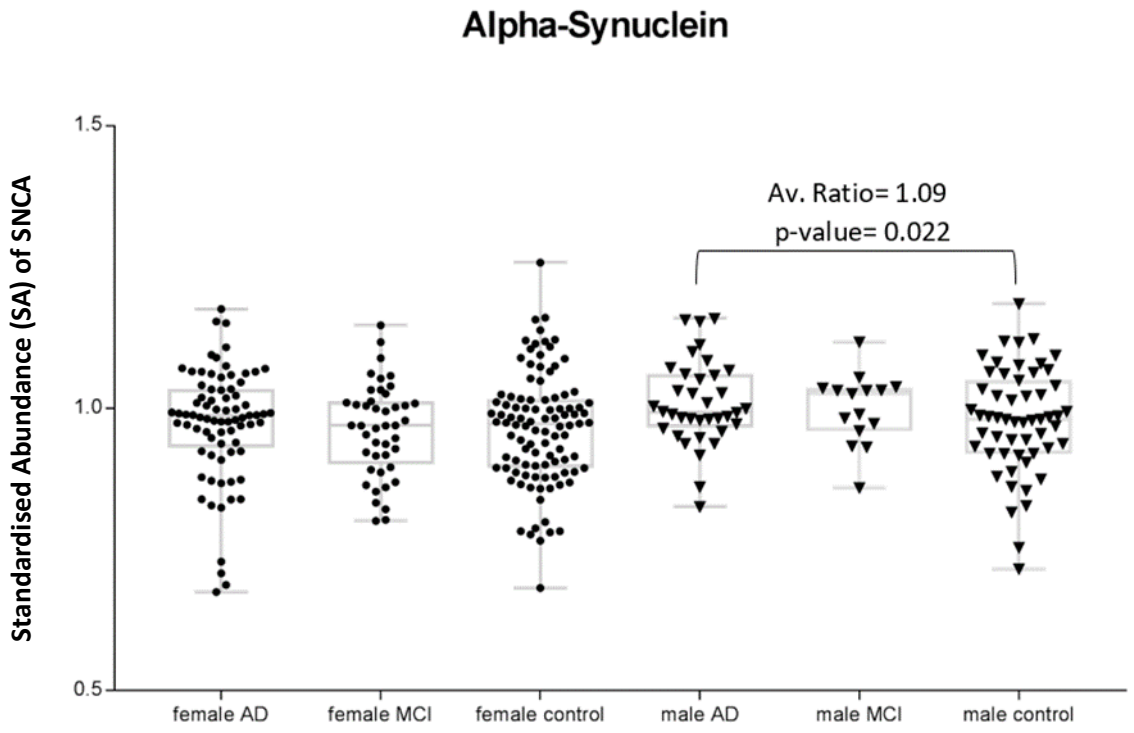

Figure 9: Effects of sex and cognition on alpha-synuclein in platelets. Protein abundances were measured by 2D-DIGE. Platelet protein levels of SNCA are depicted as SA on the y-axis. Sex differentiated AD and MCI patients, as well as their controls, are displayed in box plots. Each dot represents the SA of a single patient or control. In the box plots min/max values, median and upper/lower quartiles are displayed. The statistical significance for each group was calculated by a student t-Test using GraphPad Prism (p-value < 0.05). Only the protein levels that

fulfil the criteria are highlighted. N (AD male)= 38, N (MCI male)= 15, N (Co male)= 56, N (AD female)= 77, N (MCI female)= 44, N (Co female)= 101. AD (Alzheimer´s disease), MCI (Mild cognitive impairment).

3.3.2 A Rab GDP dissociation inhibitor alpha species with the pI 4.50 is significantly increased in male AD patients

The 2-way ANOVA showed a cognition stage-dependent (p= 0.022) change of the Rab GDP dissociation inhibitor alpha (GDI1) spot with the pI 4.50. Post hoc analysis between the particular study pairs showed a significant abundance increase of this GDI1 species in male AD patients (Av. Ratio= 1.23, p= 0.007). In females AD patients the GDI1 spot had a weaker increase with 1.11 (p= 0.043) in comparison to the female controls. However, the standardised abundance ratio was below 12% which does not fulfil the selection criteria. Furthermore, female MCI (Av. Ratio= 1.09, p= 0.254) and male MCI (Av. Ratio= 1.21, p= 0.058) were not significantly changed compared to their respective control groups.

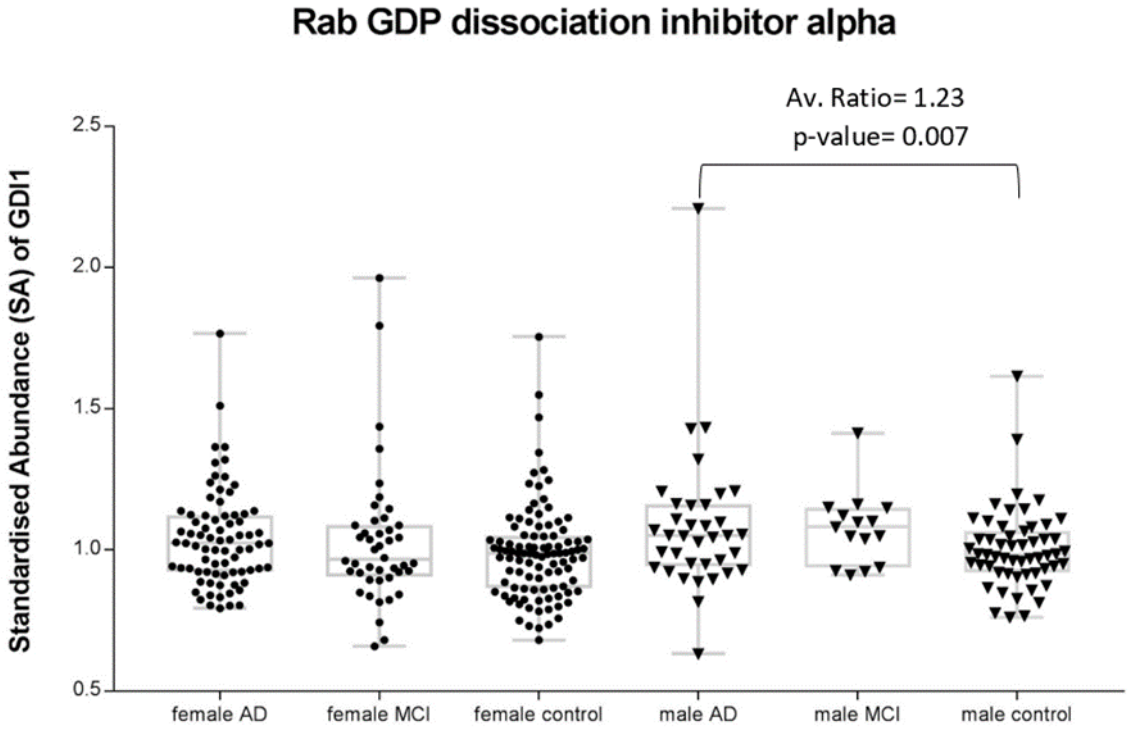

Figure 10: Effects of sex and cognition on Rab GDP dissociation inhibitor alpha species (pI 4.50) in platelets. Protein abundances were quantified by 2D-DIGE. Platelet protein levels of GDI1 are depicted as SA on the y-axis. Sex differentiated AD and MCI patients, as well as their controls, are displayed in box plots. Each dot represents the SA of a single patient or control. In the box plots min/max values, median and upper/lower quartiles are indicated. The statistical significance for each relevant study group pair was calculated by a student t-Test using GraphPad Prism (p-value < 0.05). N (AD male)= 38, N (MCI male)= 15, N (Co male)= 56, N (AD female)= 77, N (MCI female)= 44, N (Co female)= 101. AD (Alzheimer´s disease), MCI (Mild cognitive impairment).

3.3.3 Superoxide dismutase 1 is significantly increased in male AD patients

The 2-way ANOVA demonstrated a cognition stage-independent (p= 0.068) and a sex-dependent (p= 0.035) change of superoxide dismutase 1 (SOD1). The antioxidant defence member SOD1 levels were significantly increased in male AD patients (Av. Ratio= 1.24, p= 0.011) when compared to their respective control groups. In male MCI patients (Av.Ratio= 1.22, p= 0.085), female AD patients (Av.Ratio= 1.04, p= 0.544) and female MCI patients (Av.Ratio= 1.05, p= 0.526) the SOD1 abundance was not significantly changed to their respective control groups.

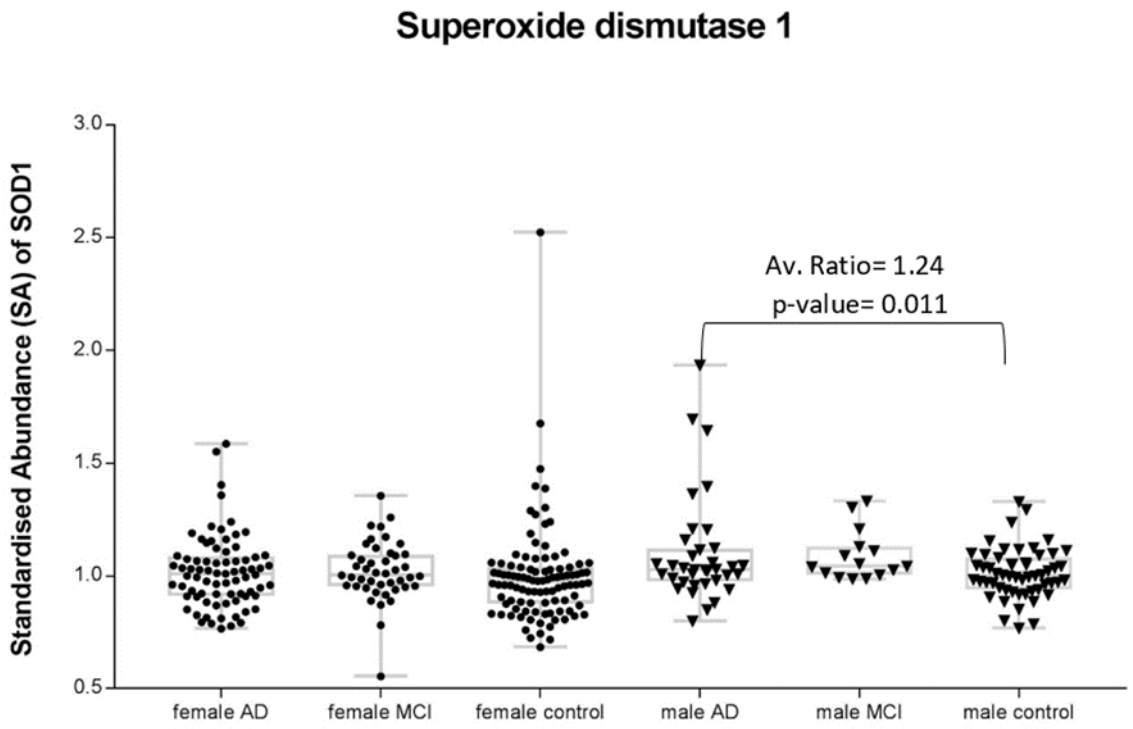

Figure 11: Effects of sex and cognition on superoxide dismutase 1 platelets. Protein abundance was analysed by 2D-DIGE. Platelet protein levels are depicted as SA on the y-axis. Sex differentiated SOD1 abundance of AD and MCI patients, as well as their controls, are illustrated in box plots. Each dot represents the SA of a single patient or control. In the box plots min/max values, median and upper/lower quartiles are displayed. The statistical significance for each group was calculated by a student t-Test using GraphPad Prism (p-value < 0.05). Only the protein levels that fulfil the criteria are highlighted. N (AD male)= 38, N (MCI male)= 15, N (Co male)= 56, N (AD female)= 77, N (MCI female)= 44, N (Co female)= 101. AD (Alzheimer´s disease), MCI (Mild cognitive impairment).

3.3.4 Glutathione peroxidase 1 is significantly decreased in AD patients of both sexes, but not in an earlier stage of impaired cognition

The 2-way ANOVA revealed a cognition stage-dependent (p= 1.2625E-08) and a sex-independent (p= 0.929) change of glutathione peroxidase 1 (GPX1). GPX1, also an antioxidant defence member showed significantly decreased protein levels in male AD patients (Av. Ratio= 0.83, p= 7.1941E-06) and female AD patients (Av. Ratio= 0.85, p= 1.7723E-07) when in comparison to their respective control groups. In contrast, the GPX1 protein abundance from female MCI (Av. Ratio= 1.00, p= 0.919) and male MCI (Av. Ratio= 1.02, p= 0.753) were not significantly changed to their respective control groups.

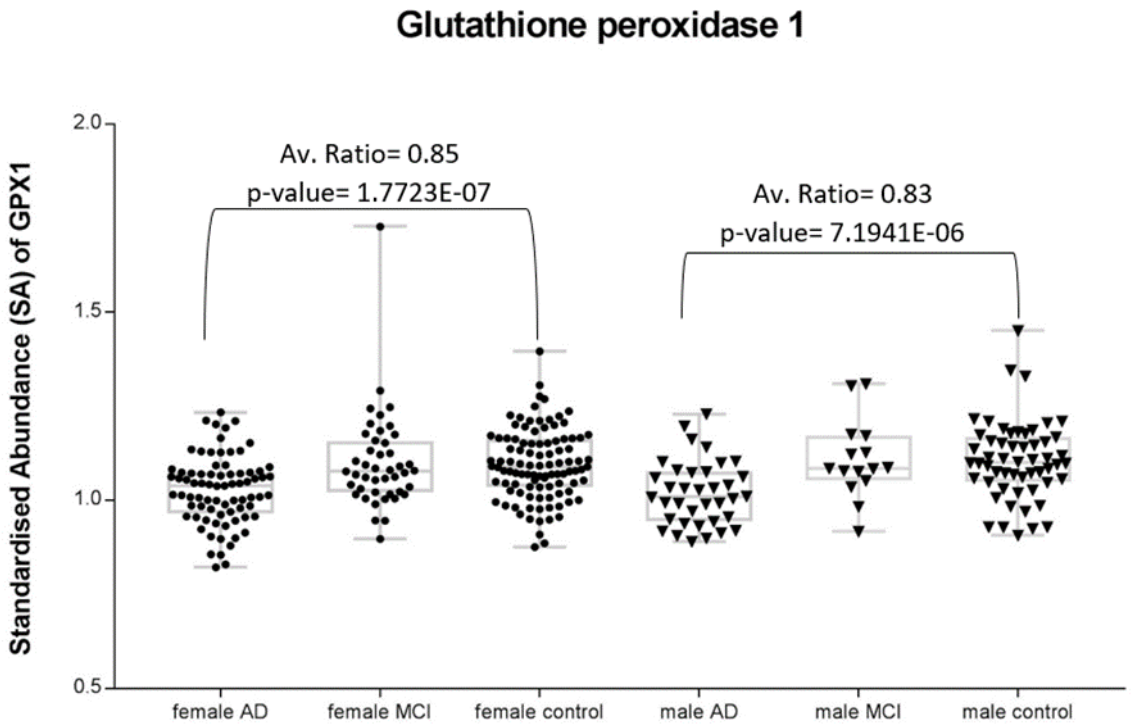

Figure 12: Effects of sex and cognition on glutathione peroxidase 1 platelets. Platelet Protein abundances were analysed by 2D-DIGE. Platelet Protein levels are depicted as SA on the y-axis. Sex differentiated GPX1 abundance from AD and MCI patients, as well as their controls, are illustrated in box plots. Each dot represents the SA of a single patient or control. In the box plots min/max values, median and upper/lower quartiles are displayed. The statistical significance for each group was calculated by a student t-Test using GraphPad Prism (p-value < 0.05). Only the protein levels that fulfil the criteria are highlighted. N (AD male)= 38, N (MCI male)= 15, N (Co male)= 56, N (AD female)= 77, N (MCI female)= 44, N (Co female)= 101. AD (Alzheimer´s disease), MCI (Mild cognitive impairment).

3.4 Identification of sex- and cognitive stage-dependent platelet protein biomarkers in the pH range 6-9

For the identification of sex- and stage-dependent protein biomarkers, the platelet proteome of patients (AD and MCI) were compared to sex- and age-matched controls. On average, 4455 protein spots were automatically detected by the DIA module of the DeCyder software, after eliminating protein spot artefacts by the DIA spot filter criteria, only including protein spots with a volume larger than “10000”. From these DIA edited 2D-DIGE maps in the pH 6-9 range group, 250-300 spots were matched manually in each Cy2 labelled 2D-DIGE image in the BVA module of the DeCyder software. Moreover, only protein matched in 80% of all 2D-DIGE gel images were statistically evaluated. According to these selection criteria, 269 protein spots were statistically analysed for sex- and cognitive stage-dependent abundance changes. The statistical significance of possible cognitive-stage and sex-dependency between the study groups (male AD/Co, male MCI/Co, female AD/Co and female MCI/Co) was calculated with a 2-way ANOVA. Afterwards, the particular significant differences between the particular study group pairs were calculated post hoc by a Student´s t-Test. Furthermore, only proteins with the standardised abundance ratio (Av. Ratio) higher than ± 12% and p-values smaller than < 0.05 were defined as eligible cognition- and sex-dependent biomarkers. Eleven proteins fulfilled these criteria and these proteins were successfully identified by MS. These proteins are depicted in Figure 13. The corresponding statistics of identified proteins are listed in Table 65.

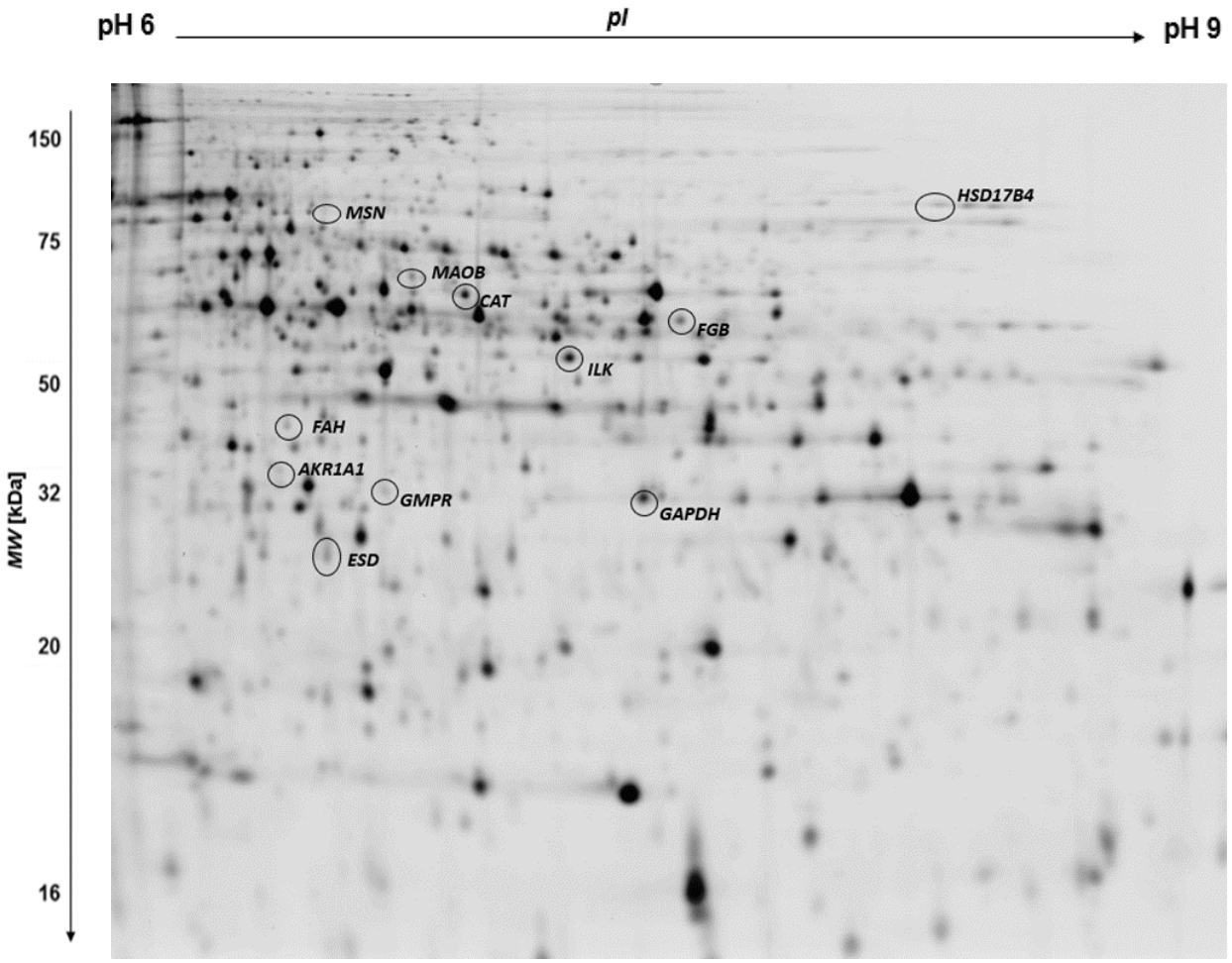

Figure 13: Representative 2D-DIGE gel in the pH range 6-9 with highlighted differentially expressed platelet proteins. CyDye-labelled proteins were separated according to their molecular weight (MW) and their isoelectric point (pI). Highlighted spots were identified by MS and are shown with their gene name on this gel. Alcohol dehydrogenase [NADP(+)] (AKR1A1), S-formylglutathione hydrolase (ESD), Moesin (MSN), Peroxisomal multifunctional enzyme type 2 (HSD17B4), Amine oxidase B (MAOB), Catalase (CAT), Fibrinogen beta Chain (FGB), Integrin-linked protein kinase1 (ILK), Fumarylacetoacetase (FAH), GMP reductase 1 (GMPR), Glyceraldehyde-3-phosphate dehydrogenase (GAPDH).

Table 65: Potential protein biomarker candidates for AD and MCI patients. Proteome analysis was performed in the pH range 6-9. Proteins of interest were selected according to the following criteria: proteins which matched in more than 80% of 2D-DIGE gels and p-value < 0.05 from independent variables (cognitive-stage and sex-differences) and interactions of 2-way ANOVA. The Av. Ratio was calculated by dividing the mean SA of each protein of each sex-defined cognitive impaired group by the corresponding mean SA of the control group. The statistical significance for each relevant study group pair was calculated by a Student´s t-Test using the Decyder™ 2D Software (p-value < 0.05). Statistical differences between the study groups were analysed using a 2-way ANOVA, main effects "cognition" and "sex", interaction term "interact". To provide a good overview the p-values of the significant proteins were labelled in different colours: male AD/MCI in blue, female AD/MCI in pink and 2-ANOVA groups (cognition, sex, interact) in orange. N (AD male)= 38, N (MCI male)= 15, N (Co male)= 56, N (AD female)= 77, N (MCI female)= 44, N (Co female)= 101. AD (Alzheimer´s disease), MCI (Mild cognitive impairment), Co (Control).

Gene name	Protein Name pH 6-9	2-ANOVA cognition	2-ANOVA sex	2 ANOVA interact	Av. Ratio male AD/Co	p-value male AD/Co	Av. Ratio female AD/Co	p-value female AD/Co	Av. Ratio male MCI/Co	p-value male MCI/Co	Av. Ratio female MCI/Co	p-value female MCI/Co
AKR1A1	Alcohol dehydrogenase [NADP(+)]	7.18E-03	0.062	0.464	1.06	0.110	1.04	0.200	1.18	3.85E-03	1.06	0.165
ESD	S-formylglutathione hydrolase	0.050	0.161	0.403	0.86	0.032	0.97	0.253	0.99	0.218	1.03	0.606
MSN	Moesin	0.139	0.991	0.252	0.99	0.853	1.02	0.447	1.00	0.857	1.19	2.51E-03
HSD17B4	Peroxisomal multifunctional enzyme type 2	0.074	0.151	0.273	1.15	0.086	1.00	0.771	0.98	0.977	0.84	0.039
MAOB	Amine oxidase B	0.074	2.56E-02	0.489	1.10	0.397	1.19	0.034	1.07	0.823	0.66	0.248
CAT	Catalase	0.102	0.580	0.942	1.02	0.742	0.97	0.822	0.99	0.313	0.80	0.030
FGB	Fibrinogen beta Chain	0.342	0.592	0.190	1.14	0.025	0.99	0.783	1.10	0.662	1.12	0.174
ILK	Integrin linked protein kinase 1	0.243	0.786	0.082	1.16	0.022	0.97	0.583	1.05	0.377	1.05	0.916
FAH	Fumarylacetoacetase	0.388	0.661	0.149	0.97	0.814	1.06	0.259	0.92	0.563	1.20	3.10E-03
GMPR	GMP reductase 1	0.056	4.68E-02	0.711	0.99	0.753	1.00	0.899	1.06	0.439	1.12	5.46E-03
GAPDH	Glyceraldehyde-3-phosphate dehydrogenase	0.221	0.728	0.493	0.97	0.797	0.77	8.40E-03	0.88	0.874	0.98	0.974

3.5 Validation of cognition and sex-related abundance of Rab GDP dissociation inhibitor alpha in platelets by WB

After characterizing the cognition and sex-dependent abundance of MS-identified GDI1 spots in platelets by 2D-DIGE, these findings were validated by a second independent method such as WB. Due to temporal restricted time of a master thesis, we decided to validate the most promising AD biomarker (GDI1) by 1D- and 2D-WB. These two kinds of WB analysis for GDI1 were performed for several reasons. We wanted to validate the MS identification of GDI1 found to have significantly higher protein levels in male AD patients. Furthermore, the anti-GDI1 antibody should identify further possible GDI1 spots in the 2D-DIGE platelet protein map. Finally, fluorescence-based semiquantitative 1D-WB analysis should verify the GDI1 abundance changes in AD and MCI patients compared to healthy controls.

3.5.1 Optimization of GDI1 detection by 1D-WB

To ensure optimal conditions for the detection and analysis of GDI1, the WB conditions had to be optimized. First, we used different amounts of platelet protein to reveal the optimal protein load and the optimal dilutions of the primary GDI1 antibody and secondary detection antibody for WB detection. After the optimisation of the WB condition (Figure 14), it was decided to use 13µg of platelet protein mixture for semiquantitative WB analysis. The optimal dilution for the primary GDI1 antibody was 1:1250 and the second fluorescence labelled antibody was 1:500.

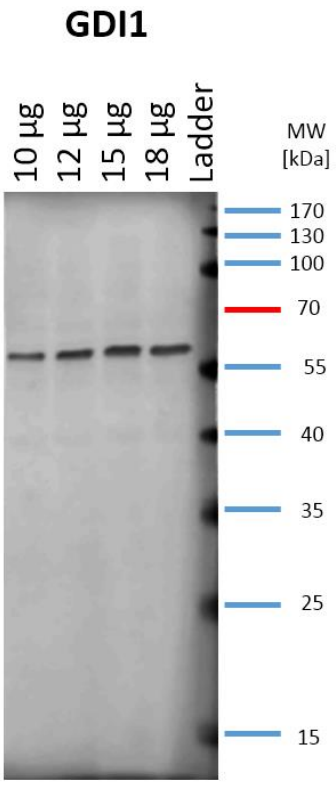

Figure 14: Optimisation of 1D-WB for GDI1 from platelets. Different amounts of platelet proteins extracts were separated on an 11.5% SDS-PAGE gel and then blotted to a nitrocellulose membrane. Subsequently, the blotted proteins on the membrane were incubated with primary- and secondary fluorescence (DyLight650) labelled antibodies. After antibody incubations, the antibody fluorescence signals were detected with a laser-assisted fluorescence scanner (Typhoon FLA 9500, GE-Healthcare). MW: molecular weight; IS: internal standard; Ladder: PageRule^{TM} Prestained Protein Ladder

3.5.2 Qualitative validation of 2D-DIGE GDI1 abundance profile by 2D-WB

A 2D-WB was performed in the pH range 4-7 to control for the MS identifications of the GDI1 protein spots. The second objective of 2D-WB analysis was to uncover further possible protein spots of GDI1 in the 2D map of platelets. Therefore, a Cy2 labelled 2D-DIGE gel was prepared and then the region of interest was blotted into a nitrocellulose membrane. Afterwards, the membrane was immunostained with antibody against GDI1. 2D-WB confirmed the MS identification of the two GDI1 protein spots (pI 4.50 and pI 5.0) and did not detected any further protein species of GDI1. The detected GDI1 spots by 2D-WB are demonstrated in Figure 15.

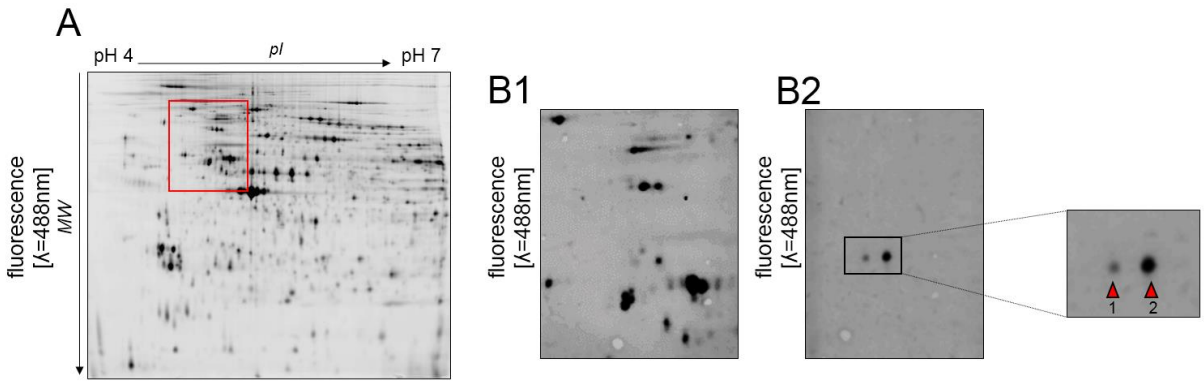

Figure 15: 2D-WB analysis of the GDI1 spots in the 2D platelet proteome map pH 4-7. 36 µg of platelet protein mix was labelled with Cy2, separated according to their pI (pH 4-7) and MW on an 11.5 % SDS-PAGE gel and blotted to a nitrocellulose membrane. Then, this membrane was immunostained with antibody against GDI1. The whole protein (Cy2) and antibody signals (Cy5) were detected with a laser-assisted fluorescence Scanner (Typhoon FLA 9500, GE-Healthcare). (A) Cy2 fluorescence of 2D-DIGE gel. (B1) Cy2 fluorescence of 2D nitrocellulose membranes. (B2) Visualisation of antibody binding on 2D-WB by fluorescent (DyLight650) labelled secondary antibody (Cy5). Detailed image of the selected area (red rectangle and B) shows the area which was cut out of the gel. Red arrows show protein spots (No. 1: pI 4.50, No. 2: pI 5.0). pI: isoelectric point; MW: molecular weight; λ: wavelength

3.5.2 Semiquantitative validation of 2D-DIGE GDI1 abundance profile by 1D-WB

To validate the 2D-DIGE characterised protein abundance alterations of GDI1 between AD-, MCI patients and controls, a semiquantitative 1D-WB analysis was performed. Therefore, platelet samples from three AD patients, three MCI patients and six matched controls were quantified by 1D-WB. The same samples were previously included in the 2D-DIGE analysis. Specific GDI1 Western blot signals were normalized by a total protein stain with tris (bathophenanthroline disulfonate) ruthenium (II) sodium salt (RuBPS), see Figure 16 A and B. Finally, the 1D-WB results were correlated to the 2D-DIGE results, see Figure 17.

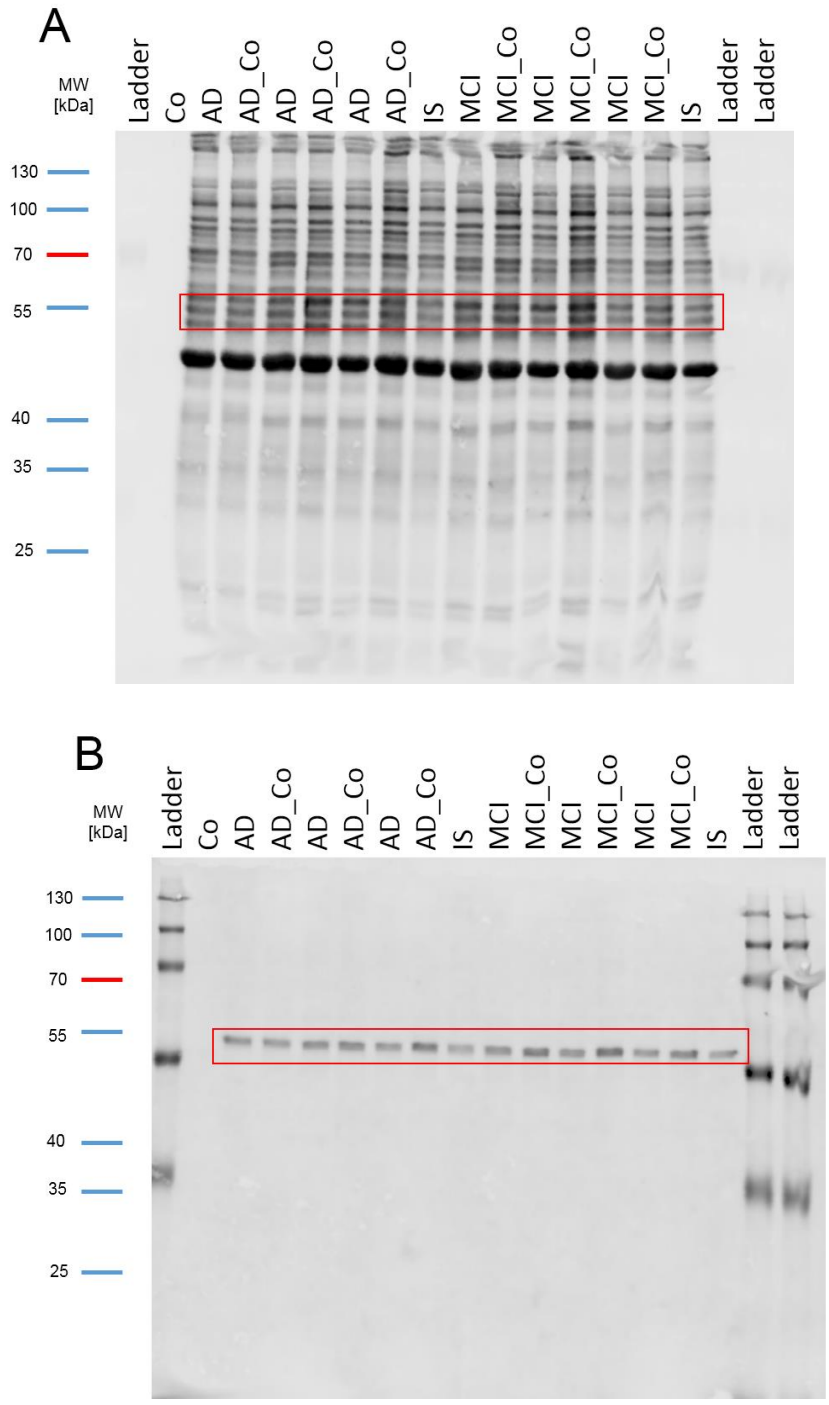

Figure 16: Validation of GDI1 levels by 1D-WB of platelet protein extract obtained from patients with AD, MCI and corresponding controls. (A) Total protein stain with RuBPS. 13 µg of platelet protein mixture of 3 AD and 3 MCI patients and corresponding control samples were loaded to an 11.5% SDS-PAGE gel. Subsequently, blotted onto a nitrocellulose membrane. Additionally, an IS for further standardization between different WBs, a protein ladder as a molecular weight standard and a negative control containing only SLAB-buffer, was applied. (B) 1D WB of GDI1. The membrane was incubated with primary and secondary antibodies to visualize GDI1 (50 kDa). Protein bands were visualised by a fluorescently labelled secondary antibody, detected with a laser-assisted fluorescence Scanner (Typhoon FLA 9500, GE-Healthcare) and quantified with 1D Image Quant Gel analysis software. AD: Alzheimer´s disease; MCI: Mild cognitive impaired; Co: control; IS: internal standard; MW: molecular weight

As previously mentioned, to ensure a good signal which is intense enough but not saturated, we decided to use 13µg of platelet protein extract for semiquantitative WB analysis. Also, it is important to mention that the GDI1 band of the 1D-WB contain both protein spots of GDI1, revealed by 2D-DIGE and 2D-WB analysis. Therefore, the SA of the two protein spots measured by 2D-DIGE had to be summarized before comparing the data. The 1D-WB results were compared to their corresponding 2D-DIGE values by the Pearson (r^2) correlation coefficient. This evaluation demonstrates no correlation (r^2=0.0026) between the 1D-WB and 2D-DIGE measured values (Figure 17).

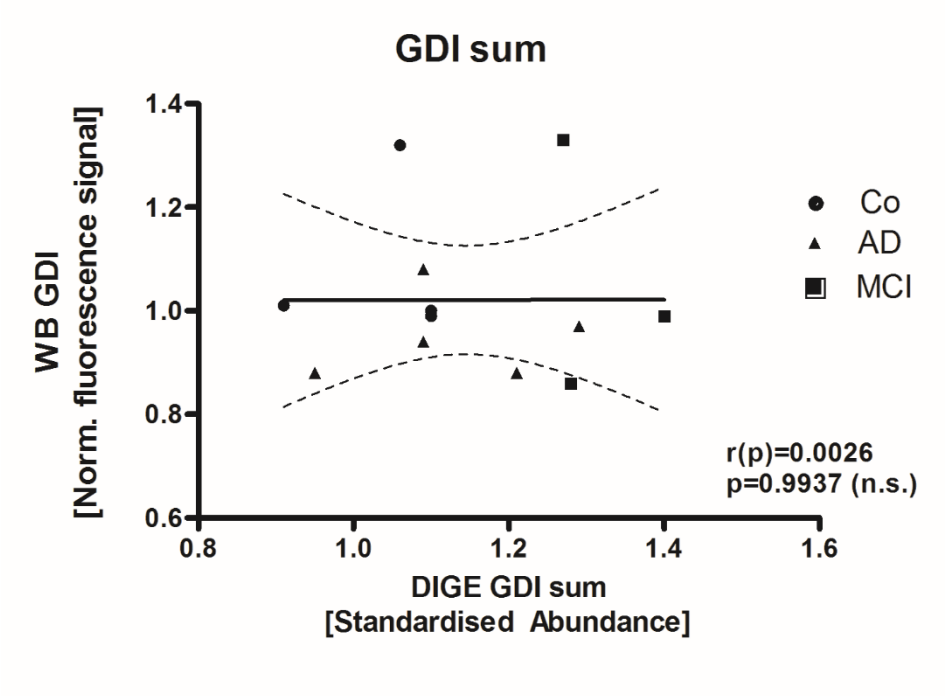

Figure 17: Validation of cognition related GDI1 platelet protein abundance by 1D WB. Scatter dot plot of 2D-DIGE and 1D-WB results. The SA of GDI1 measured by 2D-DIGE was plotted against the normalised fluorescence GDI1 signal detected by 1D-WB. The relation of protein levels (2D-DIGE vs. 1D-WB) was evaluated by the Pearson correlation coefficient (r^2). Values of patients and healthy controls are demonstrated in different geometric forms: AD (triangle) n = 3, MCI (square) n =3, Co (circle) n =6. AD: Alzheimer's disease; MCI: mild cognitive impaired.

3.6 Pathway analysis of cognition and sex-related platelet proteins

To investigate possible functional protein interactions between the identified cognition and sex-related platelet proteins from the study group pairs (male AD, female AD, male MCI and female MCI), a STRING pathway analysis was performed from significant proteins of both pH ranges (Figure 18-21). The pathway analysis revealed several significant enriched interactions between particular proteins in male AD, female AD and female MCI patients. The proteins of female AD (p= 0.0316) and MCI (p= 0.00087) patients displayed significantly more interactions than that expected from a random set of proteins of similar size, derived from the genome. In contrast to the male AD patients which had a non-significant (p= 0.051) protein-protein interaction (PPI). However, a non-significant p-value does not necessarily mean that the proteins represent a random collection. It could also indicate that the proteins are not well studied yet and their interactions are still unknown to the STRING database. In regards to male MCI patients, no protein-protein interactions or functional enrichments were found. However, as previously mentioned, still unknown interactions or the small set of proteins might also be possible reasons for this result.

(a)

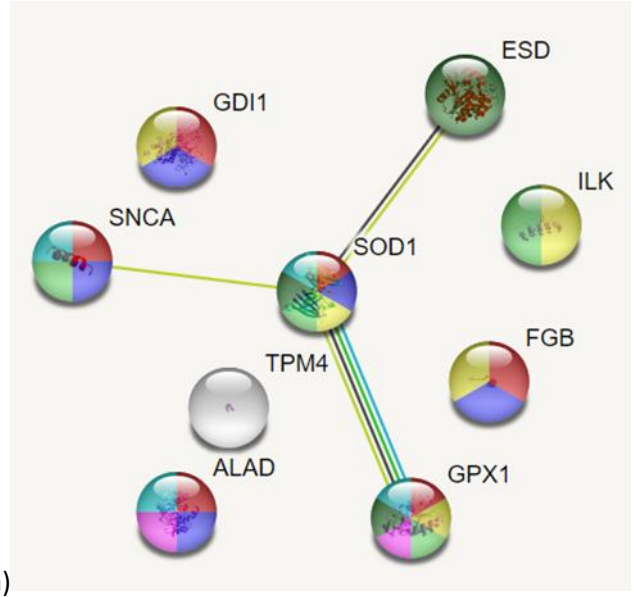

(b)

Biological Process (GO)			
GO-term	*description*	*count in gene set*	*false discovery rate*
GO:0010035	response to inorganic substance	6 of 491	2.71e-05
GO:0010038	response to metal ion	5 of 339	0.00013
GO:0090066	regulation of anatomical structure size	5 of 464	0.00040
GO:0043523	regulation of neuron apoptotic process	4 of 195	0.00042
GO:0010269	response to selenium ion	2 of 7	0.0015
GO:1990748	cellular detoxification	3 of 90	0.0016
GO:0006979	response to oxidative stress	4 of 373	0.0023

(c)

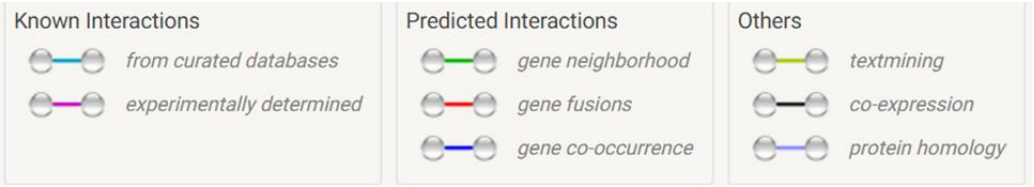

Figure 18: Pathway analysis of altered platelet proteins in male AD patients. (a) The proteins are highlighted in different colours consistent with the biological process they are involved in. (b) The biological processes and (c) the type of interactions which are indicated with different colours. Delta-aminolevulinic acid dehydratase (ALAD), Alpha-Synuclein (SNCA), Rab GDP dissociation inhibitor alpha (GDI1), Glutathione peroxidase 1 (GPX1), Superoxide dismutase 1 (SOD1), Tropomyosin alpha-4 chain (TPM4), S-formylglutathione hydrolase (ESD), Fibrinogen beta Chain (FGB), Integrin-linked protein kinase 1 (ILK). Source: STRING database; http://string-db.org/, accessed on 14th February 2020.

(a)

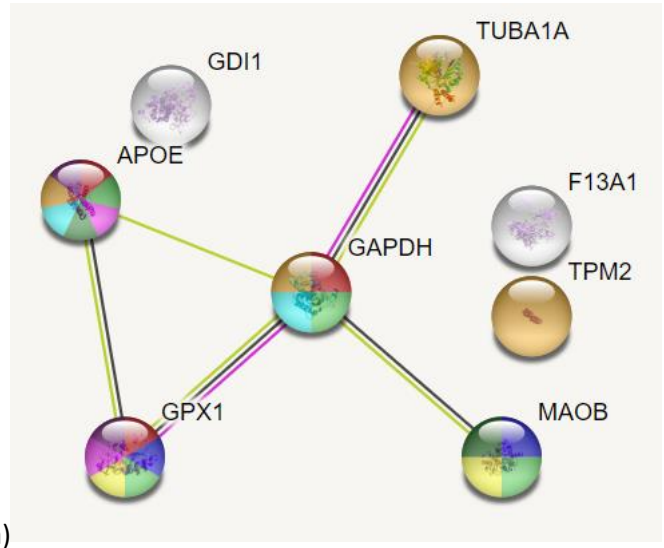

(b)

Biological Process (GO)			
GO-term	*description*	*count in gene set*	*false discovery rate*
GO:0051702	interaction with symbiont	3 of 75	0.0035
GO:0010269	response to selenium ion	2 of 7	0.0035
GO:1901361	organic cyclic compound catabolic process	4 of 484	0.0086
GO:0042743	hydrogen peroxide metabolic process	2 of 31	0.0201
GO:0042311	vasodilation	2 of 31	0.0201
GO:1901616	organic hydroxy compound catabolic process	2 of 62	0.0436
GO:0051851	modification by host of symbiont morphology or physiology	2 of 71	0.0444
GO:0007010	cytoskeleton organization	4 of 953	0.0444
GO:0006641	triglyceride metabolic process	2 of 69	0.0444

(c)

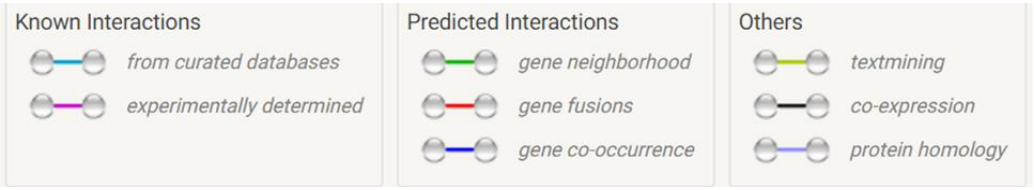

Figure 19: Pathway analysis of platelet protein changes in female AD patients. (a) The proteins are highlighted in different colours consistent with the biological process they are involved in. (b) The biological processes and (c) the type of interactions which are indicated with different colours. Tubulin alpha-3 chain (TUBA3C or TUBA1A), Tropomyosin beta chain (TPM2), Rab GDP dissociation inhibitor alpha (GDI1), Glutathione peroxidase 1 (GPX1), Coagulation factor XIII A chain precursor (F13A1), Apolipoprotein E3 precursor (APOE), Amine oxidase B (MAOB), Glyceraldehyde-3-phosphate dehydrogenase (GAPDH). Source: STRING database; http://string-db.org/, accessed on 14th February 2020.

MCI-related platelet proteins in male patients

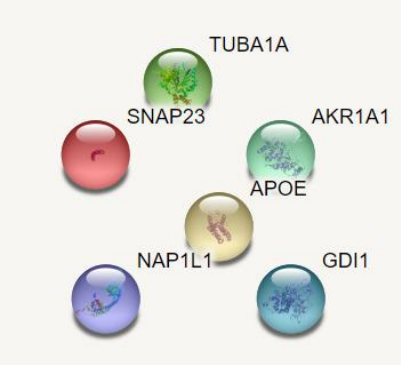

Figure 20: Pathway analysis of altered platelet proteins in male MCI patients. Tubulin alpha-3 chain (TUBA3C or TUBA1A), Rab GDP dissociation inhibitor alpha (GDI1), Nucleosome assembly protein 1-like 1 (NAP1L1), Apolipoprotein E3 precursor (APOE), Synaptosomal-associated protein 23 (SNAP23), Alcohol dehydrogenase [NADP(+)] (AKR1A1). Source: STRING database; http://string-db.org/, accessed on 14th February 2020.

MCI-related platelet proteins in females patients

(a)

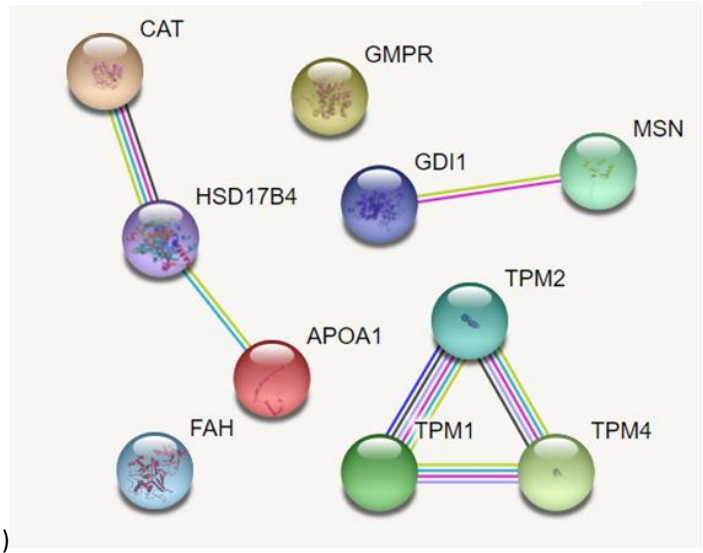

(b)

Biological Process (GO)			
GO-term	*description*	*count in gene set*	*false discovery rate*
GO:0030049	muscle filament sliding	3 of 38	0.00088
GO:0022604	regulation of cell morphogenesis	4 of 442	0.0087
GO:0007015	actin filament organization	3 of 200	0.0180
GO:0008202	steroid metabolic process	3 of 248	0.0276
GO:0051496	positive regulation of stress fiber assembly	2 of 50	0.0290
GO:0006928	movement of cell or subcellular component	5 of 1355	0.0290
GO:1901615	organic hydroxy compound metabolic process	3 of 420	0.0370
GO:0055114	oxidation-reduction process	4 of 923	0.0370

(c)

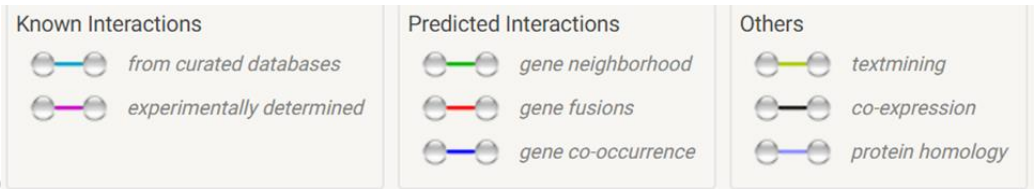

Figure 21: Pathway analysis of platelet protein changes in female MCI patients. (a) The proteins are highlighted in different colours consistent with the biological process they are involved in. (b) The biological processes and (c) the type of interactions which are indicated with different colours. Tropomyosin beta chain (TPM2), Apolipoprotein A-I precursor (APOA1), Rab GDP dissociation inhibitor alpha (GDI1), Tropomyosin alpha-4 chain (TPM4), Tropomyosin alpha-1 chain (TPM1), Moesin (MSN), Peroxisomal multifunctional enzyme type 2

(HSD17B4), Catalase (CAT), Fumarylacetoacetase (FAH), GMP reductase 1 (GMPR). Source: STRING database; http://string-db.org/, accessed on 14th February 2020.

4. Discussion

This master thesis in AD research worked on two important scientific questions. Primarily, platelets are described as a peripheral model for neurons and reflect several signs of neurological disorders [41]. These observations make them an interesting target to search for biomarkers, which could enable the development of a blood test for the diagnosis of AD. Secondarily, a sex-dependent aetiology is discussed in the pathology of AD [13, 30, 31]. Following this statement, the additional aim of this thesis was to characterise cognition and gender-related protein profiles in platelets in AD and MCI patients. Using the proteomics tools 2D-DIGE and MS, we could reveal several statistically significant cognition as well as sex-related protein abundance changes in platelets of AD and MCI patients. These findings are important molecular basics which could support the development of a blood test specific for AD, which already considers sex-related phenomenons as part of this neurodegenerative disease.

4.1 Pathway analysis of sex-and stage-dependent AD platelet protein biomarkers

Altogether we identified twenty-six significant sex- and/or cognitive stage-dependent protein changes in AD and its patients by the comparison to matched controls. STRING pathway analysis showed that in female AD patients the most significant biological process is the response to selenium ion and in the male AD patients the response to inorganic substances. Selenium is an essential nutrient and vital to the brain [68]. Selenium in the form of selenocysteine is part of selenium proteins [69] like selenoenzymes which all require selenium at their active sites for the catalytic activity, such as Glutathione peroxidases (GPx) [70]. Several studies have shown that selenium deficits cause irreparable brain injury whereas an optimal selenium intake acts protectively against cognitive decline. For example, the circulating selenium transporter selenoprotein P inhibits Aβ aggregation induced by copper. Moreover, in the presence of selenium, optimal functioning antioxidative selenoenzymes protect the neuronal cytoskeleton by inhibiting tau phosphorylation [68]. In contrast, accumulation of copper and iron in AD plaques and phosphorylated tau promote the progression of the Aβ cascade and the formation of intracellular tangles. They also facilitate the generation of ROS and subsequently the progression of tissue damage [68, 71]. Disregarding the sex-dependent cognition differences, these AD-related protein profiles are involved in the response to oxidative stress, signal transduction, vesicle-mediated transport, axonogenesis, energy metabolism, cytoskeletal regulation, nucleotide metabolism, these are all biological processes which are frequently described in neurological disorders. We selected seven from the twenty-six altered proteins for a detailed literature research in this

discussion, due to their important role generally in neurodegenerative disease and especially in AD. These proteins are Rab GDP dissociation inhibitor alpha, Alpha-synuclein, Superoxide dismutase 1, Glutathione peroxidase 1, Glyceraldehyde-3-phosphate dehydrogenase, Moesin and GMP reductase 1.

GDI1 a protein involved in vesicle-mediated transport and axonogenesis

The 2-ANOVA showed a cognitive stage-dependent (p-value=0.022) change of GDI1 species (pI 4.50) with a significant increase of GDI1 levels (23 %, p= 0.007) in the platelet proteome of male AD patients when compared to their respective controls. GDI1 has the highest protein expression in neuronal tissue [72]. The GDI1 protein family is crucial for the vesicle-trafficking machinery, especially from the ER and Golgi apparatus to other organelles. Furthermore, GDI1 delivers Rab proteins to the membrane-bound compartments and retrieve them after finishing a catalytic cycle [73, 74]. Studies have revealed that Rab proteins play an essential role in autophagic processes such as Rab5 which is essential for the early endocytic pathway and Rab7 which regulates late endosome transport [75]. Interestingly, GDI1 protein levels were also found to be significantly increased in the synaptic proteome of AD cases [63], which may suggest that this change in neurodegeneration is peripherally reflected in platelets. One quite direct functional connection with AD pathology was demonstrated in the cell model which shows that one key protein in APP processing, presenilin 1, is shown as a membrane receptor for Rab GDP dissociation inhibitor. Moreover, the abundance of GDI1 in this cell model is dependent on the protein levels of presenilin 1 [76]. A sex and cognition-related influence of GDI1 was found in X-linked non-specific mental retardation (XLMR) with a huge incidence of male patients [77]. Mutations in the human GDI1 gene [77], as well as in the GDI1-null genotype mouse model [78], are associated with memory deficits. The abundance of GDI1 was increased in the platelets of the studied male AD patient cohort. Interestingly, no difference in the abundance of the GDI1 protein level was found in patients with XLMR [77]. Nevertheless, these observations suggest that any disturbances in GDI1 phenotype may be connected to cognitive impairment, especially in male.

SNCA a potential multifunctional protein and its implication in neurodegenerative disease

We found sex-dependent changes of SNCA in LOAD patients by 2-ANOVA. Significantly elevated SNCA levels (+9%, p = 0.022) were found in the platelet proteome of LOAD male patients when compared to their respective controls. SNCA is a small intracellular presynaptic protein (140 amino acids) that exists in the balance between a soluble and a membrane-bound state. It is mainly expressed in the brain, however, it is not restricted to nervous tissue. SNCA has also been found in the muscle, kidney, liver, lung, heart, testis, blood vessels, lymphocytes, CSF, and red blood cells, blood plasma and platelets

[79]. SNCA is believed to play several roles in the regulation of synaptic vesicle release and trafficking, fatty acid-binding and neuronal survival although its functions are still under debate [80]. Misfolded and accumulated SNCA in aggregates is the major component of Lewy-bodies which is believed to play a central role in synucleinopathies. Synucleinopathies are a group of neurodegenerative disorders that includes PD, DLB, multiple systems atrophy (MSA) and pure autonomic failure (PAF) [81]. Interestingly, SNCA pathology is present in up to 50% of AD patients [61]. Several studies have revealed unchanged or slightly increased CSF SNCA levels in patients with MCI and AD. However, the higher CSF SNCA levels are positively linked with disease progression from MCI to AD and correlate negatively to cognitive performance evaluated by MMSE [82]. Some studies have found a correlation between Aβ plaques and NFTs with the cognitive status of PD dementia (PDD). A regression model study demonstrated that a combination of measures of cortical SNCA, tau, and Aβ pathologies had major predictive accuracy for dementia than every single marker alone [83]. Another large autopsy cohort regression model study showed that the inclusion of the APOε4 status enhances diagnostic accuracy for PDD in contrast to the commonly used severe cortical SNCA pathology model [84]. Moreover, the APOε4 status is associated with an increased abundance of Aβ plaques and elevated cortical and limbic SNCA pathology in PD. It is well known that APOε4 is a risk factor for LOAD, but these findings may also hint to an increased risk of dementia in PD. Additionally, high CSF levels of t-tau and p-tau were found in PDD patients, although they were not as high as in the AD patients [61]. All these findings indicate that there are copathogenic interactions between these proteins, suggesting the possible existence of a downstream mechanism on which the effects of these proteins converge [11]. There are significant sex differences between males and females in PD. Males have a higher incidence and prevalence of developing PD. Evidence has shown that an interplay between chromosomal factors and gonadal hormone factors may cause these sex differences. For example, estrogen acts neuroprotective to the dopaminergic system which is affected in PD [85]. However, investigations are needed to elucidate sex differences regarding SNCA in AD patients.

SOD1 and GPX1 as members of the antioxidant defence system

2-ANOVA analysis demonstrated a sex-dependent change (p-value= 0.035) of SOD1 levels. We found significantly increased levels (+24%, p= 0.011) of SOD1 in AD male patients in comparison to their respective controls. Parallel to our findings Choi *et al.* also found increased levels of SOD1 in the brain of AD and PD patients. Furthermore, Choi and his colleges revealed that an oxidative modification of SOD1 induces protein misfolding and accumulation which is associated with amyloid plaques and neurofibrillary tangles in AD brains [86]. In contrast to our results, other studies found no abundant changes in SOD1 between the sexes [67, 87]. In regards to the function of SOD1 and GPX1, both are

antioxidant enzymes. SOD1 (CuZnSOD) converts the superoxide radical (O_2-) into hydrogen peroxide (H_2O_2) which is then reduced by GPX1 into water (H_2O). It is crucial for normal cellular function that a balance is maintained between ROS production and the antioxidant defence [12, 66, 67]. A 2-ANOVA analysis revealed a stage-dependent change (p-value= 1.2625E-08) of GPX1 levels. We found significantly decreased levels in AD male patients (-17%, p= 7.1941E-06) and AD female patients (-15%, p= 1.7723E-07) when in comparison to their respective controls. Parallel to our findings Puertas *et al.* found also decreased levels of GPX1 in the plasma of AD patients in both genders. The significant decrease of GPX1 levels in AD patients might occur as a result of increased levels of ROS, leading to rapid consumption of antioxidant enzymes [67]. An additional explanation could be metal dyshomeostasis which facilitates ROS production [68, 71], and deficiency of selenium which is required for optimal functioning of GPX1 [68, 70]. As a consequence, the antioxidant defence system is insufficient to protect the cell against oxidative damage which may promote the development of pathological changes, and therefore neurodegeneration [67]. There is sufficient evidence that the activity of antioxidant enzymes is altered in AD although there are discrepancies regarding the levels of SOD1 and GPX1 in red blood cells and serum [66, 88-94]. Porcellotti and colleagues investigated age-dependent (3 months, 6 months, 9 months, 12 months and 18 months) alterations of SOD1 and GPX1 in the neocortex of AD model mice, with the distribution of Aβ peptides and oligomers by WB and IHC. The enzymatic activity of SOD1 and GPX1 was downregulated in the young age (3m), upregulated in the adult age (9m, 12m) and again downregulated in the mature age (18m). Results which may reveal the genesis, progression and development of AD, which at its late-stage leads to the irreversible loss of the antioxidant enzymes [95]. These findings pinpoint that alteration of antioxidant enzymes levels are age- and stage-dependent which might elucidate the cause of discrepancies between studies.

Glyceraldehyde-3-phosphate dehydrogenase (GAPDH) a ubiquitous protein

We found significantly decreased levels of GAPDH in AD female patients (-23%, p= 8.40E-03) when compared to their respective controls. Mazzola *et al.* also reported a decrease of 27% of the GAPDH function in nuclear and post-nuclear fractions of fibroblast cells of AD patients when compared to their respective controls [96]. GAPDH is an essential glycolytic enzyme which is also involved in many other cellular processes such as nuclear functions (DNA replication and repair, nuclear RNA transport), redox post-translational modifications, membrane transport and binds to important small molecules such as glutathione (GSH), p53, ribozymes and nitric oxide (NO). Recent studies indicate implications of GAPDH in AD pathology by its interaction and development of complexes with Aβ and APP [97]. Moreover, further studies have demonstrated that tau interacts with GAPDH promoting its inactivation. These results indicate an involvement of GAPDH in the aggregation of Aβ and tau, suggesting that GAPDH

might be a suitable biomarker for diagnosis of AD [97]. In regards to sex differences, GAPDH reveals a complex pattern which still needs to be clarified in AD. GAPDH is regulated independently by hormones at various developmental stages and tissues. For example, estradiol upregulates GAPDH mRNA concentrations in endometrium but downregulates them in the liver. However, the mRNA levels in the brain (hypothalamus and cortex) are regulated developmentally [98-100].

Moesin (MSN) a key player in the cytoskeletal regulation

We found increased levels of moesin in MCI female patients (19%, p= 2.51E-03) when compared to their respective controls. Interestingly, in contrast to our results, González-Sánchez and colleagues found significantly decreased levels of moesin in the platelet proteome of AD patients when compared to their respective controls [101]. Moesin is a member of the ezrin-radixin-moesin (ERM) family which play an essential role in the regulation of the cytoskeleton. Furthermore, they are involved in the membrane transport, signal transduction and immune mediation [102-104]. In regards to sex differences, a study group investigated how progesterone acts on actin remodelling in rat cortical neurons. They found that progesterone enhances the formation of dendritic spines by increasing the phosphorylation of moesin and mediating its migration to cell membrane sites where spines are formed. On the other hand, silencing of moesin revokes the positive effects of progesterone on the dendritic spines of neurons. Nevertheless, progesterone seems to rapidly induce changes in neuronal cell morphology indicating the essential role of sex steroids (estrogen and progesterone) in neuronal plasticity and transmission and by acting protectively against neurodegenerative diseases [105]. These findings indicate that the cytoskeletal proteins might be compromised in AD, leading to changes in the cytoskeletal dynamics and impaired cellular functions linked to moesin. However, further investigations will be needed to elucidate how sex- and stage-dependent differences influence the expression and function of moesin in AD.

GMP reductase 1 (GMPR) an essential enzyme for the nucleotide metabolism

The 2-ANOVA showed a sex-dependent (p-value= 4.68E-02) change of GMPR levels. We found a significant increase of GMPR levels (12%, p= 5.46E-03) in the platelet proteome of female MCI patients when compared to their respective controls. GMPR is a highly conserved enzyme, from bacteria to humans, that plays a crucial role in the cytosolic nucleotide metabolism. GMPR catalyzes irreversibly the NADPH-dependent deamination of guanosine monophosphate (GMP) into inosine monophosphate (IMP) and ammonium which enables the synthesis of purine nucleotides, ATP generation, and transcriptional signalling [106, 107]. Liu and colleagues found a link between GMPR

gene expression and a gradual increase in AD progression. AD patients show an increased expression of the GMPR gene in contrast to the respective controls. Furthermore, GMPR is linked to the AMPK and adenosine receptor-mediated pathways, both leading to tau phosphorylation. The logical consequence suggests that an increase of the GMPR levels would lead to increased tau phosphorylation and facilitate AD progression. The ability of GMPR to classify AD cases and its direct association with tau phosphorylation makes it a promising diagnostic biomarker and therapeutic target [107]. To date, no literature involving sex-related differences in the protein levels of GMPR in AD has been found. Future investigation will be needed to elucidate this topic.

5. Conclusion

Multiple sex- and cognitive stage-specific platelet-derived biomarkers were identified in this masters thesis. These findings provide data for the development of an accurate prognostic and diagnostic blood biomarker panel that could help develop more effective drug treatments and to achieve a personalized medical approach. The promising AD biomarkers are involved in signal transduction, vesicle-mediated transport and axonogenesis (GDI1), co-pathogenic interactions with APOε4, Aβ and tau (SNCA), antioxidant activity (SOD1 and GPX1), energy metabolism (GAPDH), cytoskeletal regulation (MSN) and nucleotide metabolism (GMPR). Additionally, STRING pathway analysis showed a relation of selenium deficiency and metal dyshomeostasis to irreparable tissue damage and progressive cognitive decline. Our results reconfirm the extremely complicated molecular pathology of AD and its multifactorial nature. To date, no disease-modifying treatments are available, and the diagnosis of the disease is complicated. To establish an accurate diagnosis a variety of approaches and detection methods which are invasive (CSF sample analysis) and expensive (PET) are needed. Therefore, future research in the discovery and validation of biomarkers in the preclinical phase of AD from peripheral biofluids is of immense importance and provides a great opportunity to aid in the successful treatment of this incurable disease.

6. References

1. Drouin, E. and G. Drouin, *The first report of Alzheimer's disease.* Lancet Neurol, 2017. **16**(9): p. 687.
2. Lane, C.A., J. Hardy, and J.M. Schott, *Alzheimer's disease.* Eur J Neurol, 2018. **25**(1): p. 59-70.
3. Hickman, R.A., A. Faustin, and T. Wisniewski, *Alzheimer Disease and Its Growing Epidemic: Risk Factors, Biomarkers, and the Urgent Need for Therapeutics.* Neurol Clin, 2016. **34**(4): p. 941-953.
4. *2016 Alzheimer's disease facts and figures.* Alzheimers Dement, 2016. **12**(4): p. 459-509.
5. Niu, H., et al., *Prevalence and incidence of Alzheimer's disease in Europe: A meta-analysis.* Neurología (English Edition), 2017. **32**(8): p. 523-532.
6. *World Alzheimer Report 2018.* 2018.
7. Nichols, E., et al., *Global, regional, and national burden of Alzheimer's disease and other dementias, 1990–2016: a systematic analysis for the Global Burden of Disease Study 2016.* The Lancet Neurology, 2019. **18**(1): p. 88-106.
8. *Global, regional, and national age–sex specific all-cause and cause-specific mortality for 240 causes of death, 1990–2013: a systematic analysis for the Global Burden of Disease Study 2013.* The Lancet, 2015. **385**(9963): p. 117-171.
9. Selkoe, D.J. and J. Hardy, *The amyloid hypothesis of Alzheimer's disease at 25 years.* EMBO Mol Med, 2016. **8**(6): p. 595-608.
10. Tilley, L., K. Morgan, and N. Kalsheker, *Genetic risk factors in Alzheimer's disease.* Molecular pathology : MP, 1998. **51**(6): p. 293-304.
11. Huang, Y. and L. Mucke, *Alzheimer mechanisms and therapeutic strategies.* Cell, 2012. **148**(6): p. 1204-22.
12. Tonnies, E. and E. Trushina, *Oxidative Stress, Synaptic Dysfunction, and Alzheimer's Disease.* J Alzheimers Dis, 2017. **57**(4): p. 1105-1121.
13. Laws, K.R., K. Irvine, and T.M. Gale, *Sex differences in Alzheimer's disease.* Curr Opin Psychiatry, 2018. **31**(2): p. 133-139.
14. Kivipelto, M., et al., *Midlife vascular risk factors and Alzheimer's disease in later life: longitudinal, population based study.* Bmj, 2001. **322**(7300): p. 1447-51.
15. Vieira, M.N.N., R.A.S. Lima-Filho, and F.G. De Felice, *Connecting Alzheimer's disease to diabetes: Underlying mechanisms and potential therapeutic targets.* Neuropharmacology, 2018. **136**(Pt B): p. 160-171.
16. Vijayan, M. and P.H. Reddy, *Stroke, Vascular Dementia, and Alzheimer's Disease: Molecular Links.* J Alzheimers Dis, 2016. **54**(2): p. 427-43.
17. Durazzo, T.C., et al., *Smoking and increased Alzheimer's disease risk: a review of potential mechanisms.* Alzheimers Dement, 2014. **10**(3 Suppl): p. S122-45.
18. Bachhuber, T., et al., *Inhibition of amyloid-β plaque formation by α-synuclein.* Nature Medicine, 2015. **21**: p. 802.
19. Atik, A., T. Stewart, and J. Zhang, *Alpha-Synuclein as a Biomarker for Parkinson's Disease.* Brain Pathol, 2016. **26**(3): p. 410-8.
20. Higgins, J.H.a.G., *Alzheimer's Disease: The Amyloid Cascade Hypothesis.* 1992.
21. Deyts, C., G. Thinakaran, and A.T. Parent, *APP Receptor? To Be or Not To Be.* Trends Pharmacol Sci, 2016. **37**(5): p. 390-411.
22. Šerý, O., et al., *Molecular mechanisms of neuropathological changes in Alzheimer's disease: a review.* Folia Neuropathologica, 2013. **1**: p. 1-9.
23. Amemori, T., et al., *Alzheimer's Disease: Mechanism and Approach to Cell Therapy.* Int J Mol Sci, 2015. **16**(11): p. 26417-51.

24. Sanabria-Castro, A., I. Alvarado-Echeverría, and C. Monge-Bonilla, *Molecular Pathogenesis of Alzheimer's Disease: An Update.* Annals of Neurosciences, 2017. **24**(1): p. 46-54.
25. Wu, X.L., et al., *Tau-mediated Neurodegeneration and Potential Implications in Diagnosis and Treatment of Alzheimer's Disease.* Chin Med J (Engl), 2017. **130**(24): p. 2978-2990.
26. Hu, W., et al., *Expression of Tau Pathology-Related Proteins in Different Brain Regions: A Molecular Basis of Tau Pathogenesis.* Front Aging Neurosci, 2017. **9**: p. 311.
27. Zhang, X., et al., *The Early Events That Initiate beta-Amyloid Aggregation in Alzheimer's Disease.* Front Aging Neurosci, 2018. **10**: p. 359.
28. Schaffer, C., et al., *Biomarkers in the Diagnosis and Prognosis of Alzheimer's Disease.* J Lab Autom, 2015. **20**(5): p. 589-600.
29. *Bhushan I, Kour M, Kour G, et al. Alzheimer's disease: Causes and treatment – A review. Ann Biotechnol. 2018; 1(1): 1002.*
30. Dumitrescu, L., et al., *Sex Differences in the Genetic Architecture of Alzheimer's Disease.* Curr Genet Med Rep, 2019. **7**(1): p. 13-21.
31. Ferretti, M.T., et al., *Sex differences in Alzheimer disease - the gateway to precision medicine.* Nat Rev Neurol, 2018. **14**(8): p. 457-469.
32. Jack, C.R., Jr., et al., *Introduction to the recommendations from the National Institute on Aging-Alzheimer's Association workgroups on diagnostic guidelines for Alzheimer's disease.* Alzheimers Dement, 2011. **7**(3): p. 257-62.
33. Dubois, B., et al., *Advancing research diagnostic criteria for Alzheimer's disease: the IWG-2 criteria.* The Lancet Neurology, 2014. **13**(6): p. 614-629.
34. Umlauf, E., et al., *Careful neuropsychological testing reveals a novel genetic marker, GSTO1*C, linked to the pre-stage of Alzheimer's disease.* Oncotarget, 2016. **7**(26): p. 39108-39117.
35. Norris, D., M.S. Clark, and S. Shipley, *The Mental Status Examination.* Am Fam Physician, 2016. **94**(8): p. 635-641.
36. Fillenbaum, G.G., et al., *Consortium to Establish a Registry for Alzheimer's Disease (CERAD): the first twenty years.* Alzheimers Dement, 2008. **4**(2): p. 96-109.
37. Chandler, M.J., et al., *A total score for the CERAD neuropsychological battery.* Neurology, 2005. **65**(1): p. 102-6.
38. *Bhushan I, Kour M, Kour G, et al. Alzheimer's disease: Causes and treatment – A review. Ann Biotechnol. 2018; 1(1): 1002.*
39. Jack, C.R., Jr. and D.M. Holtzman, *Biomarker modeling of Alzheimer's disease.* Neuron, 2013. **80**(6): p. 1347-58.
40. Molinuevo, J.L., et al., *Current state of Alzheimer's fluid biomarkers.* Acta Neuropathol, 2018. **136**(6): p. 821-853.
41. Veitinger, M., et al., *Platelets, a reliable source for peripheral Alzheimer's disease biomarkers?* Acta Neuropathol Commun, 2014. **2**: p. 65.
42. Gowert, N.S., et al., *Blood platelets in the progression of Alzheimer's disease.* PLoS One, 2014. **9**(2): p. e90523.
43. Donovan, L.E., et al., *Exploring the potential of the platelet membrane proteome as a source of peripheral biomarkers for Alzheimer's disease.* Alzheimers Res Ther, 2013. **5**(3): p. 32.
44. Mills, E.W., R. Green, and N.T. Ingolia, *Slowed decay of mRNAs enhances platelet specific translation.* Blood, 2017. **129**(17): p. e38-e48.
45. Chen, M., et al., *Platelets are the primary source of amyloid beta-peptide in human blood.* Biochem Biophys Res Commun, 1995. **213**(1): p. 96-103.
46. Kim, S.H., et al., *Beyond symptomatic effects: potential of donepezil as a neuroprotective agent and disease modifier in Alzheimer's disease.* Br J Pharmacol, 2017. **174**(23): p. 4224-4232.
47. Mendiola-Precoma, J., et al., *Therapies for Prevention and Treatment of Alzheimer's Disease.* Biomed Res Int, 2016. **2016**: p. 2589276.

48. Yiannopoulou, K.G. and S.G. Papageorgiou, *Current and future treatments for Alzheimer's disease.* Therapeutic Advances in Neurological Disorders, 2012. **6**(1): p. 19-33.
49. Reumiller, C.M., et al., *Gender-related increase of tropomyosin-1 abundance in platelets of Alzheimer's disease and mild cognitive impairment patients.* J Proteomics, 2018. **178**: p. 73-81.
50. Winblad, B., et al., *Mild cognitive impairment--beyond controversies, towards a consensus: report of the International Working Group on Mild Cognitive Impairment.* J Intern Med, 2004. **256**(3): p. 240-6.
51. Groscurth, P., et al., *Effects of washing and gel filtration on the ultrastructure of human platelets.* Acta Haematol, 1987. **77**(3): p. 150-5.
52. Lindon, J.N., R. Rodvien, and D.F. Waugh, *Effects of matrix contact during gel filtration of human platelets in plasma.* Thromb Haemost, 1976. **36**(2): p. 311-8.
53. Bradford, M.M., *A rapid and sensitive method for the quantitation of microgram quantities of protein utilizing the principle of protein-dye binding.* Anal Biochem, 1976. **72**: p. 248-54.
54. Alban, A., et al., *A novel experimental design for comparative two-dimensional gel analysis: two-dimensional difference gel electrophoresis incorporating a pooled internal standard.* Proteomics, 2003. **3**(1): p. 36-44.
55. *Beckett P. (2012) The Basics of 2D DIGE. In: Cramer R., Westermeier R. (eds) Difference Gel Electrophoresis (DIGE). Methods in Molecular Biology (Methods and Protocols), vol 854. Humana Press.*
56. Lam, T.C., et al., *Application of fluorescence difference gel electrophoresis technology in searching for protein biomarkers in chick myopia.* J Proteome Res, 2007. **6**(11): p. 4135-49.
57. Wu, Y., et al., *Early quantitative profiling of differential retinal protein expression in lens-induced myopia in guinea pig using fluorescence difference two-dimensional gel electrophoresis.* Mol Med Rep, 2018. **17**(4): p. 5571-5580.
58. Chevallet, M., S. Luche, and T. Rabilloud, *Silver staining of proteins in polyacrylamide gels.* Nat Protoc, 2006. **1**(4): p. 1852-8.
59. Taylor, S.C. and A. Posch, *The design of a quantitative western blot experiment.* Biomed Res Int, 2014. **2014**: p. 361590.
60. MacPhee, D.J., *Methodological considerations for improving Western blot analysis.* J Pharmacol Toxicol Methods, 2010. **61**(2): p. 171-7.
61. Irwin, D.J., V.M. Lee, and J.Q. Trojanowski, *Parkinson's disease dementia: convergence of alpha-synuclein, tau and amyloid-beta pathologies.* Nat Rev Neurosci, 2013. **14**(9): p. 626-36.
62. Zare-Shahabadi, A., et al., *Autophagy in Alzheimer's disease.* Rev Neurosci, 2015. **26**(4): p. 385-95.
63. Chang, R.Y., et al., *The synaptic proteome in Alzheimer's disease.* Alzheimers Dement, 2013. **9**(5): p. 499-511.
64. Li, Q., Y. Liu, and M. Sun, *Autophagy and Alzheimer's Disease.* Cell Mol Neurobiol, 2017. **37**(3): p. 377-388.
65. Salminen, A., et al., *Impaired autophagy and APP processing in Alzheimer's disease: The potential role of Beclin 1 interactome.* Prog Neurobiol, 2013. **106-107**: p. 33-54.
66. Bermejo, P., et al., *Peripheral levels of glutathione and protein oxidation as markers in the development of Alzheimer's disease from Mild Cognitive Impairment.* Free Radic Res, 2008. **42**(2): p. 162-70.
67. Puertas, M.C., et al., *Plasma oxidative stress parameters in men and women with early stage Alzheimer type dementia.* Exp Gerontol, 2012. **47**(8): p. 625-30.
68. Aaseth, J., et al., *Treatment strategies in Alzheimer's disease: a review with focus on selenium supplementation.* Biometals, 2016. **29**(5): p. 827-39.
69. Kurokawa, S. and M.J. Berry, *Selenium. Role of the essential metalloid in health.* Met Ions Life Sci, 2013. **13**: p. 499-534.
70. Roy, G., et al., *Selenium-containing enzymes in mammals: Chemical perspectives.* Journal of Chemical Sciences, 2005. **117**(4): p. 287-303.

71. Bonda, D.J., et al., *Role of metal dyshomeostasis in Alzheimer's disease.* Metallomics, 2011. **3**(3): p. 267-70.
72. Bachner, D., et al., *Expression patterns of two human genes coding for different rab GDP-dissociation inhibitors (GDIs), extremely conserved proteins involved in cellular transport.* Hum Mol Genet, 1995. **4**(4): p. 701-8.
73. Baskys, A., et al., *Rab-mediated endocytosis: linking neurodegeneration, neuroprotection, and synaptic plasticity?* Ann N Y Acad Sci, 2007. **1122**: p. 313-29.
74. Ezaki, B. and E. Nakakihara, *Possible involvement of GDI1 protein, a GDP dissociation inhibitor related to vesicle transport, in an amelioration of zinc toxicity in Saccharomyces cerevisiae.* Yeast, 2012. **29**(1): p. 17-24.
75. Ao, X., L. Zou, and Y. Wu, *Regulation of autophagy by the Rab GTPase network.* Cell Death Differ, 2014. **21**(3): p. 348-58.
76. Scheper, W., et al., *Alzheimer's presenilin 1 is a putative membrane receptor for rab GDP dissociation inhibitor.* Hum Mol Genet, 2000. **9**(2): p. 303-10.
77. D'Adamo, P., et al., *Mutations in GDI1 are responsible for X-linked non-specific mental retardation.* Nat Genet, 1998. **19**(2): p. 134-9.
78. More, L., et al., *Altered fronto-striatal functions in the Gdi1-null mouse model of X-linked Intellectual Disability.* Neuroscience, 2017. **344**: p. 346-359.
79. Burre, J., M. Sharma, and T.C. Sudhof, *Cell Biology and Pathophysiology of alpha-Synuclein.* Cold Spring Harb Perspect Med, 2018. **8**(3).
80. Bousset, L., et al., *Structural and functional characterization of two alpha-synuclein strains.* Nat Commun, 2013. **4**: p. 2575.
81. Villar-Pique, A., T. Lopes da Fonseca, and T.F. Outeiro, *Structure, function and toxicity of alpha-synuclein: the Bermuda triangle in synucleinopathies.* J Neurochem, 2016. **139 Suppl 1**: p. 240-255.
82. Twohig, D. and H.M. Nielsen, *α-synuclein in the pathophysiology of Alzheimer's disease.* Molecular neurodegeneration, 2019. **14**(1): p. 23-23.
83. Compta, Y., et al., *Lewy- and Alzheimer-type pathologies in Parkinson's disease dementia: which is more important?* Brain : a journal of neurology, 2011. **134**(Pt 5): p. 1493-1505.
84. Irwin, D.J., et al., *Neuropathologic substrates of Parkinson disease dementia.* Ann Neurol, 2012. **72**(4): p. 587-98.
85. Smith, K.M. and N. Dahodwala, *Sex differences in Parkinson's disease and other movement disorders.* Exp Neurol, 2014. **259**: p. 44-56.
86. Choi, J., et al., *Oxidative modifications and aggregation of Cu,Zn-superoxide dismutase associated with Alzheimer and Parkinson diseases.* J Biol Chem, 2005. **280**(12): p. 11648-55.
87. Chico, L., et al., *Oxidative stress and APO E polymorphisms in Alzheimer's disease and in mild cognitive impairment.* Free Radic Res, 2013. **47**(8): p. 569-76.
88. Kawamoto, E.M., et al., *Oxidative state in platelets and erythrocytes in aging and Alzheimer's disease.* Neurobiol Aging, 2005. **26**(6): p. 857-64.
89. Kharrazi, H., et al., *Association between enzymatic and non-enzymatic antioxidant defense mechanism with apolipoprotein E genotypes in Alzheimer disease.* Clin Biochem, 2008. **41**(12): p. 932-6.
90. Rossi, L., et al., *Red blood cell copper, zinc superoxide dismutase activity is higher in Alzheimer's disease and is decreased by D-penicillamine.* Neurosci Lett, 2002. **329**(2): p. 137-40.
91. Vural, H., et al., *Alterations of plasma magnesium, copper, zinc, iron and selenium concentrations and some related erythrocyte antioxidant enzyme activities in patients with Alzheimer's disease.* J Trace Elem Med Biol, 2010. **24**(3): p. 169-73.
92. Padurariu, M., et al., *Changes of some oxidative stress markers in the serum of patients with mild cognitive impairment and Alzheimer's disease.* Neurosci Lett, 2010. **469**(1): p. 6-10.
93. Torres, L.L., et al., *Peripheral oxidative stress biomarkers in mild cognitive impairment and Alzheimer's disease.* J Alzheimers Dis, 2011. **26**(1): p. 59-68.

94. Cristalli, D.O., et al., *Peripheral markers in neurodegenerative patients and their first-degree relatives.* J Neurol Sci, 2012. **314**(1-2): p. 48-56.
95. Porcellotti, S., et al., *Oxidative Stress during the Progression of beta-Amyloid Pathology in the Neocortex of the Tg2576 Mouse Model of Alzheimer's Disease.* Oxid Med Cell Longev, 2015. **2015**: p. 967203.
96. Mazzola, J.L. and M.A. Sirover, *Reduction of glyceraldehyde-3-phosphate dehydrogenase activity in Alzheimer's disease and in Huntington's disease fibroblasts.* J Neurochem, 2001. **76**(2): p. 442-9.
97. El Kadmiri, N., et al., *Glyceraldehyde-3-phosphate dehydrogenase (GAPDH) and Alzheimer's disease.* Pathol Biol (Paris), 2014. **62**(6): p. 333-6.
98. Perrot-Sinal, T.S., A.M. Davis, and M.M. McCarthy, *Developmental sex differences in glutamic acid decarboxylase (GAD(65)) and the housekeeping gene, GAPDH.* Brain Res, 2001. **922**(2): p. 201-8.
99. Lustig, R.H., et al., *Ontogeny, sex dimorphism, and neonatal sex hormone determination of synapse-associated messenger RNAs in rat brain.* Brain Res Mol Brain Res, 1993. **20**(1-2): p. 101-10.
100. Zou, K. and N.H. Ing, *Oestradiol up-regulates oestrogen receptor, cyclophilin, and glyceraldehyde phosphate dehydrogenase mRNA concentrations in endometrium, but down-regulates them in liver.* J Steroid Biochem Mol Biol, 1998. **64**(5-6): p. 231-7.
101. Gonzalez-Sanchez, M., et al., *Platelet Proteomic Analysis Revealed Differential Pattern of Cytoskeletal- and Immune-Related Proteins at Early Stages of Alzheimer's Disease.* Mol Neurobiol, 2018. **55**(12): p. 8815-8825.
102. Satooka, H., et al., *The ERM Protein Moesin Regulates CD8(+) Regulatory T Cell Homeostasis and Self-Tolerance.* J Immunol, 2017. **199**(10): p. 3418-3426.
103. Takahashi, K., et al., *Direct interaction of the Rho GDP dissociation inhibitor with ezrin/radixin/moesin initiates the activation of the Rho small G protein.* J Biol Chem, 1997. **272**(37): p. 23371-5.
104. Vaheri, A., et al., *The ezrin protein family: membrane-cytoskeleton interactions and disease associations.* Curr Opin Cell Biol, 1997. **9**(5): p. 659-66.
105. Sanchez, A.M., et al., *Effects of progesterone and medroxyprogesterone on actin remodeling and neuronal spine formation.* Mol Endocrinol, 2013. **27**(4): p. 693-702.
106. Sommerville, E.W., et al., *Identification of a novel heterozygous guanosine monophosphate reductase (GMPR) variant in a patient with a late-onset disorder of mitochondrial DNA maintenance.* Clin Genet, 2019.
107. Liu, H., K. Luo, and D. Luo, *Guanosine monophosphate reductase 1 is a potential therapeutic target for Alzheimer's disease.* Sci Rep, 2018. **8**(1): p. 2759.

Figure references:

Exemplary picture for western blot wet transfer sandwich available at: https://www.sinobiological.com/category/wb-wet-transfer, accessed on 16th April 2020.

Protein pathway analysis generated with STRING database available at: https://string-db.org/, accessed on 14th February 2020.

University of Vienna logo available at: https://public.univie.ac.at/logos/, accessed on 24th January 2020.

“Ich habe mich bemüht, sämtliche Inhaber der Bildrechte ausfindig zu machen und ihre Zustimmung zur Verwendung der Bilder in dieser Arbeit eingeholt. Sollte dennoch eine Urheberrechtsverletzung bekannt werden, ersuche ich um Meldung bei mir.“

“I have endeavoured to find all image right owners to obtain their consent to use their images in this master thesis. In case of copyright infringement, however, I request the establishment takes up contact with me.”

VI. LIST OF FIGURES

VII. LIST OF TABLES

VIII. LIST OF FORMULAS